DESIGN OPTIMIZATION OF FLWHEEL BASED

ENERGY STORAGE SYSTEM

PROJECT FINAL REPORT

for

MAE 598: Design Optimization

Project by: Vishal Chandrasekhar

Victor Vincent Sanjai

Mohammad Hejazi

Naga Abhishek

8th MAY 2015

Abstract

Flywheels are being used as energy storage systems for years but were not fully exploited due to weight factor. With the advent of composite materials that problem is now resolved resulting in flywheels being used in commercial vehicles in the near future as a replacement heavy weigh KERS systems.

FLYBRID KERS is a technology which will be very prominently used in the future because of its high efficiency and lower cost compared to other energy storage systems. Thus, we as a group were intrigued to study about this technology and tried to improve its efficiency by modifying certain aspects of this technology. FLYBRID KERS is a very sophisticated technology which is being used in F-1 cars, hence even a small increase in efficiency is a sufficient improvement.

Our project deals with the optimization of the energy storage in the flywheel of a FLYBRID KERS. The overall system is fragmented into four individual subsystems which have their own objective functions and constraints and are optimized individually. The four subsystems considered are:

- Maximizing Kinetic energy of the flywheel by improving moment of inertia
- Minimizing Stator-Rotor losses in the flybrid
- Minimizing coupling losses in the flybrid
- Minimizing mechanical losses in the flybrid

Table of Contents

1. Introduction

FLYBRID KERS is a type of Kinetic Energy Recovery system where instead of a battery a mechanical flywheel is used. The system aims at storing the energy lost due to braking and use it to aid in accelerating the vehicle later. This is done by a flywheel which is a metal/composite disk rotating at very high speed and stores rotational energy. Flybrid Technology Systems uses Flywheel based Kinetic Energy Recovery System (KERS). In conventional KERS, system battery and other associated systems are used, but this uses a new low weight flywheel system which delivers greater power and has higher fuel efficiency than electronic systems. This technology might be the answer to stringent pollution control norms of the future and to meet high energy/power conversion needs.

The flywheel hybrid system for road cars is expected to offer 20% CO2 fuel savings under New European Driving Cycle test conditions, and up to 30% in real-world conditions. It is a reliable and efficient replacement for Battery. Designed to last 250,000 km, this technology makes it possible to store more energy during short braking periods, dramatically increasing system effectiveness. The system is very efficient with up to 70% of braking energy being returned to the wheels to drive the vehicle back up to speed. Flybrid KERS technology is around 1/3 the cost of an equivalent power electric hybrid system.

2. Overall Design Problem Statement

Our overall design objective is to maximize the kinetic energy storage in the flywheel of a FLYBRID KERS system. In order to do that we have chosen four individual subsystems related to the flywheel design. By optimizing these subsystems individually we aim to maximize the kinetic energy storage in the flywheel by minimizing the losses in the flybrid which are the stator rotor losses due to the magnetic bearings, losses in the coupling due to vibrations when energy is transmitted from the CVT to the flywheel and mechanical losses due frictional and aerodynamic force.

The flywheel kinetic energy storage optimization including the minimization of the flywheel losses can be done by optimizing the geometry of the flywheel. As the flywheel volume increases the energy storage increases but the flywheel structure has certain volume constraints as it is kept inside a casing and also there are other geometric trade-offs between the subsystems which have to be feasibly and optimally balanced to achieve an overall system optimum.

3. Nomenclature

Symbol	Description	Unit
Ro	Outer Radius of the Flywheel	meter
Ri	Inner Radius of the Flywheel	meter
r	Radius of the shaft	meter
t_w	Thickness of the web	meter
H	Length of the Flywheel	meter
L	Rotor Length	meter
d_{so}	Stator Outer Diameter	meter
x1	Split Ratio	constant
x2	Aspect Ratio	constant
d	Distance from the web surface to the top most part of the flywheel	meter
c	Damping Coefficient	N.m/rad
k	Spring Constant	Kg.m2/s
μ	Poisson's Ratio	constant
ω	Angular Velocity	rad/sec
ρ	Density of the material	kg/m3
v	Tip Velocity	m/s
I_1	Polar moment of inertia of the flywheel	kg.m2
I_{p1}	Polar moment of inertia of the web	kg.m2
I_{p2}	Polar moment of inertia of the rim	kg.m2
m_1	Mass of the web	kg
m_2	Mass of the rim	kg
S_y	Safe Yield Stress	MPa
τ	Applied Torque	N.m
I_2	Moment of inertia of the CVT	kg.m2

4.   Subsystems optimization

4.1 Design Optimization of the Structural Subsystem of the Flywheel

4.1.1 Introduction

Flywheel design is a key aspect for designing and developing a flywheel energy storage system. The flywheel rotor has high speed working conditions and hence must possess high energy density, high specific energy, low weight, low density and high mechanical strength properties. The flywheel must be designed to withstand the radial and tangential stresses acting on it. The flywheel design should take into account the geometry of the flywheel casing and the geometry of the shaft. The material chosen for the flywheel is Aluminum 7050 as it has low weight and possesses good load bearing capacity. The goal of the design process is to achieve the optimum geometric parameters of the flywheel and the factors to be considered for this process are energy storage, operational speeds, material behavior, moment of inertia and the general configuration of the flywheel.

4.1.2 Problem statement

The objective of this subsystem is to maximize the kinetic energy storage in the flywheel by maximizing the moment of inertia of the flywheel. For this subsystem, the kinetic energy stored in the flywheel is maximized without considering the energy losses, once the energy losses due to vibration, stator-rotor losses and the mechanical losses are calculated from the other subsystems, they are integrated with the structural subsystem and the net kinetic energy stored in the flywheel is calculated. The moment of inertia of the flywheel is maximized by maximizing the polar moment of inertia equation of the flywheel. The constraints such as stress constraints, volume constraints and linear geometric constraints are used while solving the optimization problem.
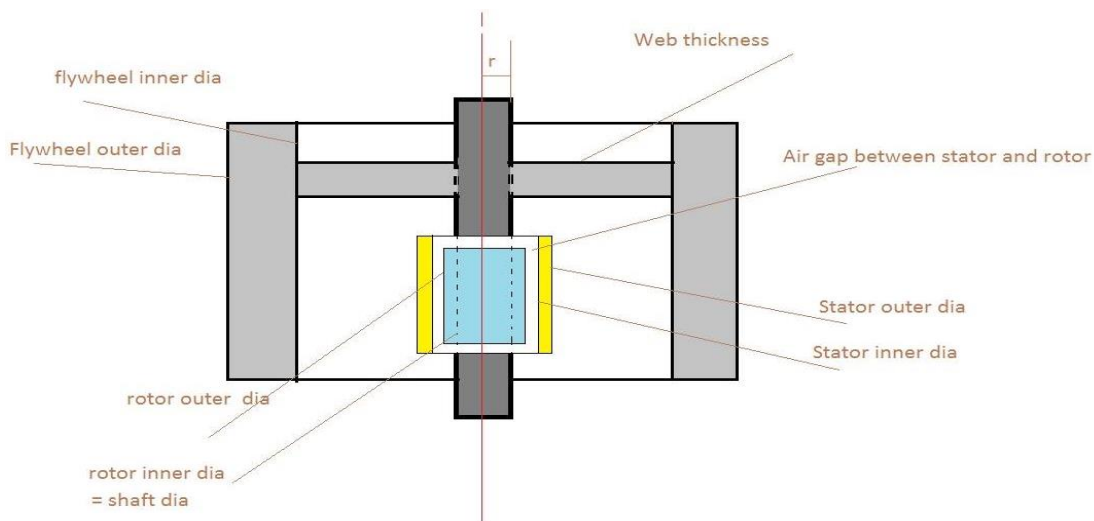

Figure 1 - Flywheel Design

Material Properties for Aluminum 7050

Density (kg/m3)	Poisson's Ratio (μ)	Safe Yield Stress(Sy) (MPa)
2810	0.33	455

<div align="center">Table 1- Material properties of Aluminum 7050</div>

4.1.3 Mathematical Model

4.1.3.1 Design Variables

R_i : Inner radius of the flywheel (m)

R_o : Outer radius of the flywheel (m)

r   : radius of the shaft (m)

t_w: Web thickness (m)

H: Length of the flywheel (m)

4.1.3.2 Design Parameters

μ- Poisson's Ratio

ω- Angular velocity of the flywheel (rad/sec)

ρ- Material density (kg/m3)

v- Tip velocity of the flywheel (m/s)

4.1.3.3 Objective Function

The objective is to maximize the kinetic energy stored in the flywheel and since the moment of inertia of the flywheel is directly proportional to the kinetic energy stored, it is necessary to maximize the moment of inertia stored in the flywheel.

The flywheel geometry can be divided into spoke and rim geometry and they are considered to be a uniform thickness rotating disc respectively. So the moment of inertia equation for a cylinder is considered. The moment of inertia of the flywheel is dependent on the polar moment of inertia and is taken to be the sum of the moment of inertia of the rim and the moment of inertia of the web.

The Kinetic energy stored in the flywheel, $KE = \frac{1}{2} I_1 [\omega_{max}^2 - \omega_{min}^2]$

I_1 – Moment of inertia of the flywheel
ω- Angular velocity of the flywheel

Maximize $f = \frac{1}{2} I_1 [\omega_{max}^2 - \omega_{min}^2]$

Polar Moment of inertia

The Moment of inertia equation consists of two parts, the pol

$$I_1 = I_{p1} + I_{p2} = \frac{m_1}{2}(r^2 + R_i^2) + \frac{m_2}{2}(R_i^2 + R_o^2)$$
$$= \frac{\rho \pi t_w}{2}(R_i^4 - r^4) + \frac{\rho \pi H}{2}(R_o^4 - R_i^4)$$

I_1 – Polar moment of inertia of the flywheel (kg.m2)

I_{p1} – Polar moment of inertia of the web (kg.m2)

I_{p2} – Polar moment of inertia of the rim (kg.m2)

m_1 – Mass of the web (kg)

m_2 – Mass of the rim (kg)

4.1.3.4 Constraints

Stress constraint based on Tresca failure criterion for isotropic materials

$$g1: \frac{3+\mu}{4}\rho\omega2\left(R_o^2 + \frac{1-\mu}{3+\mu}r^2\right) < [S_y]$$

The packaging volume of the flywheel system including the flywheel casing is taken to 18 liters

$$g2: \pi R_o^2 H - 0.018 = 0$$

Optimum radius ratio calculated using energy density and specific energy equations

$$g3: \frac{R_i}{R_o} = 0.49$$

Geometric Constraints

$$g4: R_i - R_o \leq 0$$

$$g5: 0.25H - t_w \leq 0$$

$$g6: t_w - 0.33H \leq 0$$

$$g7: R_i - r - 0.052 \leq 0$$

4.1.4 Model Analysis

4.1.4.1 Stress Constraint based on the Tresca failure criterion

The stress at a point in the disc is three stress states: the radial stress σr, tangential stress σt, and axial stress σz. Because the surface of the disc is a free surface in the z direction, σz =0. Since the material used is isotropic in nature, the Tresca failure criterion is used as the stress condition. According to this criterion,

σ1 −σ3 ≤ [S$_y$]

Where σ1 and σ3 are the maximum and minimum principal stresses and [Sy] is the safe yield stress of the material. The radial and the tangential stresses are the principal stresses for this system. The radial and the tangential stresses are the principal stresses for this system.

For an isotropic material,

Radial stress,

$$\sigma_r = \frac{3+\mu}{8}\rho\omega 2\left[R_o^2 + r^2 - \frac{R_o^2 r^2}{r_i^2} - r_i^2\right] \tag{1}$$

Tangential stress,

$$\sigma_t = \frac{3+\mu}{8}\rho\omega 2\left[R_o^2 + r^2 + \frac{R_o^2 r^2}{r_i^2} - \frac{1+3\mu}{3+\mu}\ r_i^2\right] \tag{2}$$

where,

r$_i$ – radius of the ith point

μ- Poisson's Ratio

ω- Angular velocity

ρ- Material density

The maximum radial stress is at ri = $\sqrt{R_o r}$ in Eq.(1) and the maximum tangential stress is at r$_i$ =r in Eq.(2)

$$\sigma_{rmax} = \frac{3+\mu}{8}\rho\omega 2\ (R_o - r\ )^2 \tag{4}$$

$$\sigma_{tmax} = \frac{3+\mu}{4}\rho\omega 2\left(R_o^2 + \frac{1-\mu}{3+\mu}\ r^2\right) \tag{5}$$

Comparing the tangential stress σ_{ti} with the maximum radial stress σ_{rmax} at r$_i$ = $\sqrt{R_o r}$ point, we get,

$$\sigma_{ti} - \sigma_{rmax} = \frac{3+\mu}{8}\rho\omega^2\left[R_o^2 + r^2 + \frac{1-\mu}{3+\mu}2R_or\right] - \frac{3+\mu}{8}\rho\omega^2\,(R_o - r\,)^2 \;>0 \tag{- (6)}$$

Comparing the radial stress σ_{ri} with the maximum tangential stress σ_{tmax} at ri = r and ri = Ro, the radial stress is σ_{ri}=0 when ri = r and ri = Ro in Equation (1), the maximum stress is always at the inner radius. Thus we get,

$$\sigma1 - \sigma3 = \sigma_{tmax} = \frac{3+\mu}{4}\rho\omega^2\left(R_o^2 + \frac{1-\mu}{3+\mu}r^2\right) < [S_y] \tag{7}$$

Equation (7) gives the maximum stress acting at any given point in the flywheel which acts as a constraint equation for the system.

From Equation (7),

$$\text{Ro} < \sqrt{\frac{1}{3+\mu}\left[\frac{4[Sy]}{\rho\omega^2} - (1-\mu)r^2\right]} \tag{8}$$

Equation (8) gives a constraint relation between the outer radius of the flywheel and the radius of the shaft.

4.1.4.2 Optimum Radius ratio based on Energy density and Specific energy calculations

Using the energy density and the specific energy equations, an optimum radius ratio can be obtained. High energy density and specific energy values are desired, thus using their respective equations a good balance of energy density and the specific energy values are obtained with respect to the radius ratio (R_i/R_o). The maximum tip velocity 'v' of the flywheel is substituted in the equations and a plot is generated using MATLAB to obtain an optimum radius ratio.

$$\text{Energy Density} = \frac{\text{Energy Stored in the Flywheel Rim}}{\text{Rim Enclosed Volume}}$$

$$= \frac{\rho v^2}{4}[1\text{-}(R_i/R_o)^4]$$

$$\text{Specific Energy} = \frac{\text{Energy Stored in the Flywheel Rim}}{\text{Mass of the Rim}}$$

$$= \frac{v^2}{4}[1\text{-}(R_i/R_o)^2]$$
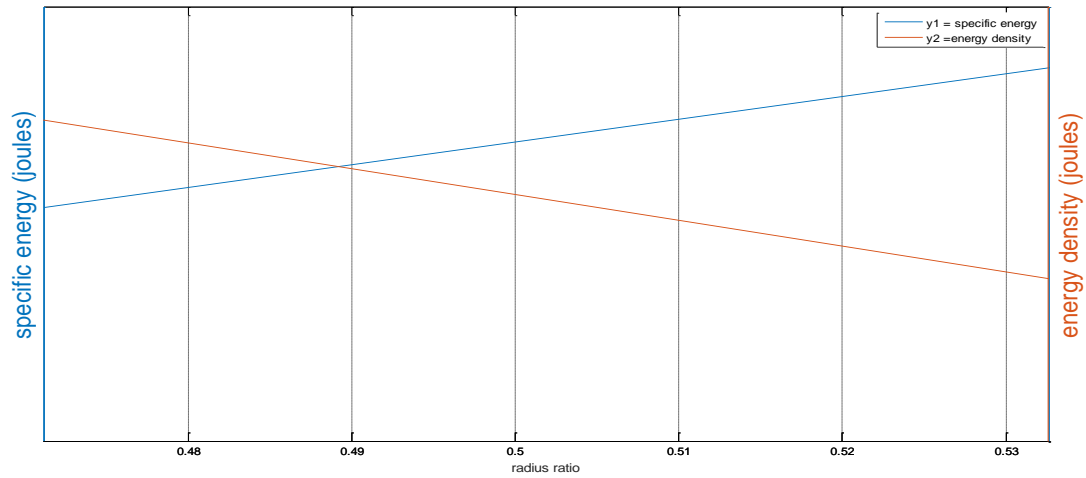
Figure 2- Plot showing the variation of the radius ratio with respect to the specific energy and energy density of the flywheel

The plot comparing the radius ratio with the specific energy and energy density is shown in Figure2. From the plot it can be seen that at a radius ratio of 0.49, the two curves meet. The energy density value obtained is 398 MJ and the specific energy value obtained is 359.8 KJ. These values are taken as optimum values and the radius ratio of 0.49 is used as a constraint in maximizing the moment of inertia equation.

4.1.4.3 Pre-optimization visualization of influence of inner and outer radius on the Moment of inertia of the flywheel

Figure 3- Contour Plot showing the variation of the moment of inertia of the flywheel with respect to its inner and outer radius

8

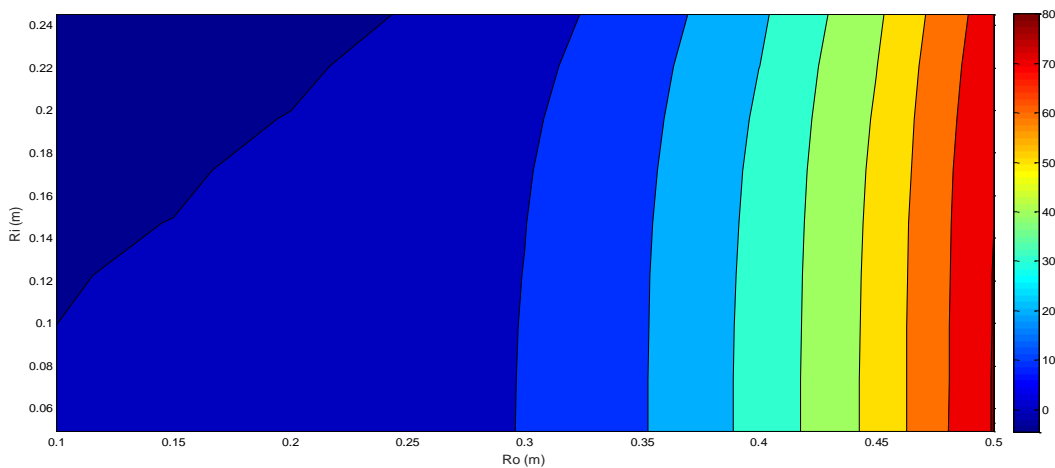A contour plot determining the relationship between the inner and outer radius and the moment of inertia is shown in Figure 3. The X-axis represents the outer radius and the Y-axis represents the inner radius. A larger moment of inertia can be obtained at higher radius values but due to the mass constraint which is explained in detail in the next plot, a maximum inner radius of 0.08m and a maximum outer radius of 0.2m can only be chosen.
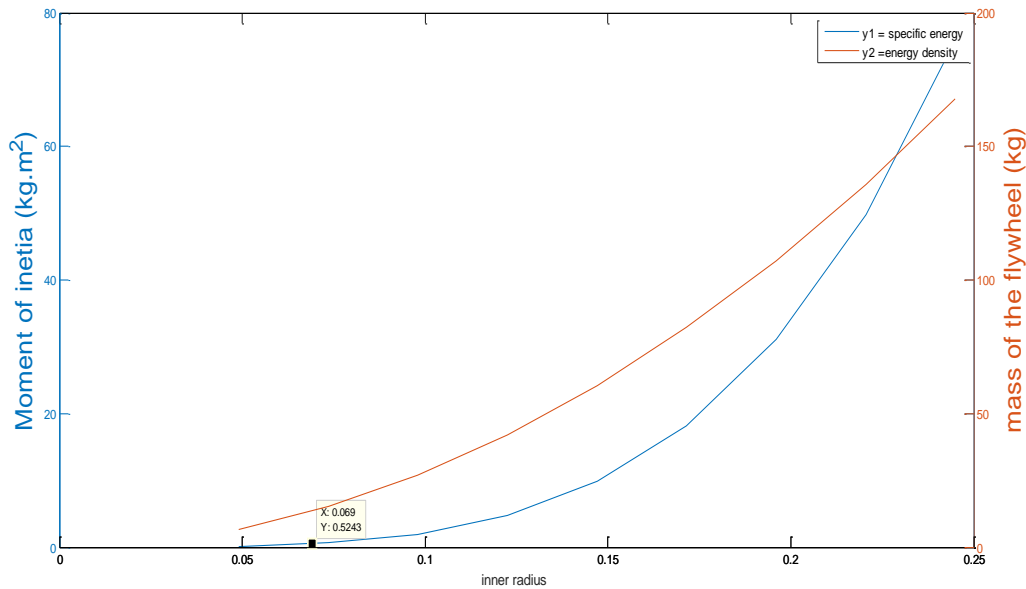

Figure 4- Plot showing the variation of the moment of inertia of the flywheel with respect to the inner radius and mass of the flywheel

In order to understand the relationship between the Moment of inertia of the flywheel, mass of the flywheel and the radius ratio, a plot is made with the inner radius as the X-axis, Moment of inertia as the left Y-axis and the mass of the flywheel as the right Y-axis. The plot is shown in Figure 4. As the inner radius increases the moment of inertia of the flywheel increases, but it has to be constrained within a feasible mass of the flywheel. From our literature review we found that the feasible mass of the flywheel ranges from 10 to 20 kg, thus taking it into account, it can be seen from the graph that the best inner radius value is 0.069 m and the corresponding moment of inertia value is 0.524 kg.m2 and the corresponding flywheel mass value is 13.55 kg. These values help us understand the relation between the flywheel geometry and the moment of inertia of the flywheel. This was used as a base for proceeding with the flywheel design optimization.

The outer radius of the flywheel (Ro) is one of the common variables with the mechanical losses subsystem of the flywheel, according to the objective function of the mechanical losses subsystem Ro must be minimized to reduce the drag coefficient but the objective function of the structural subsystem requires a high Ro thus this acts as a trade-off.

4.1.4.4 Monotonicity table

$f = \frac{\rho \pi x_4}{2}(x_1^4 - x_3^4) + \frac{\rho \pi x_5}{2}(x_2^4 - x_1^4)$

$g1: \frac{3+\mu}{4} \rho \omega 2 \left(x_2^2 + \frac{1-\mu}{3+\mu} x_3^2 \right) < [Sy]$

$g4: x_1 - x_2 \leq 0$

$g5: 0.25x_5 - x_4 \leq 0$

$g6: x_4 - 0.33x_5 \leq 0$

$g7: x_1 - x_3 - 0.052 \leq 0$

	x1 (Ri)	x2 (Ro)	x3 (r)	x4 (tw)	x5 (H)
f	-	+	-	+	+
g1		+	+		
g4	+	-			
g5				-	+
g6				+	-
g7	+		-		

Table 2- Monotonicity Table

4.1.4.5 Active Constraints

w.r.t 'x1' g4 and g7 are active

w.r.t 'x2' g4 is active

w.r.t 'x3' g1 is active

w.r.t 'x4' g5 is active

w.r.t 'x4' g6 is active

g2 and g3 are equality constraints
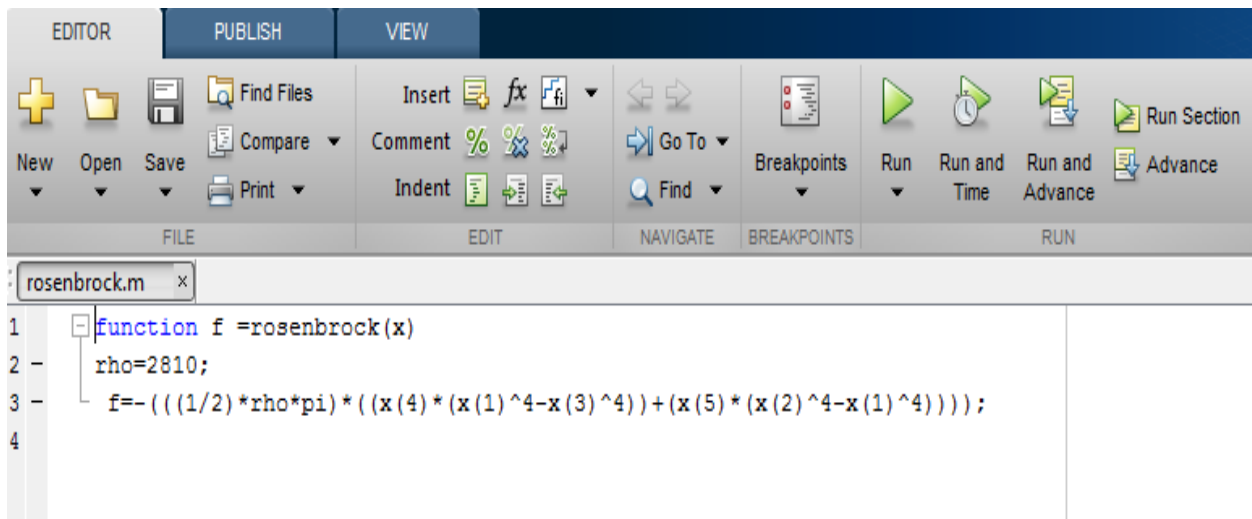
4.1.5 Optimization study and Results

4.1.5.1 Lower and Upper bounds of the Design Variables

Variables	Lower Bound	Upper Bound
R_i	0	inf
R_o	0	inf
r	0.02	inf
t_w	0	inf
H	0	inf

Table 3- Upper and Lower bounds of the design variables

If a lower bound is not given to the shaft radius it goes to zero, this is because the maximum stress acts at the inner radius of the flywheel thus in order to compensate it, the flywheel becomes a solid cylinder rather than a hollow one. Thus a lower bound is given to the shaft radius to maintain the geometry of a hollow flywheel.

4.1.5.2 Objective function and nonlinear constraint equations in Matlab


```
function f =rosenbrock(x)
rho=2810;
f=-(((1/2)*rho*pi)*((x(4)*(x(1)^4-x(3)^4))+(x(5)*(x(2)^4-x(1)^4))));
```

Figure 5- Matlab file for the objective function

Figure-5 shows a Matlab script which was created to enter the objective function, where f is the moment of inertia equation which is written in the negative null form.

```matlab
function [c,ceq] = unitdisk(x)
  mu=0.33;
    omega=3141.59;
   rho=2810;

  c=[((((3+mu)/4)*(rho*((omega)^2))*((x(2)^2+((1-mu)/(3+mu))*x(3)^2)))-455000000)];
  ceq=[x(5)*pi*(((x(2))^2))-0.018];
```

Figure 6- Matlab file for the non-linear constraint equations

Figure-6 shows a Matlab file which was created to input the non-linear constraints, the non-linear inequality constraint is the stress constraint and the non-linear equality constraint is the volume constraint.

4.1.5.3 Optimization Toolbox

The optimization was done using the Matlab Optimization Toolbox. The fmincon solver is used and the algorithms used to solve the optimization problem were SQP and Active Set algorithms.
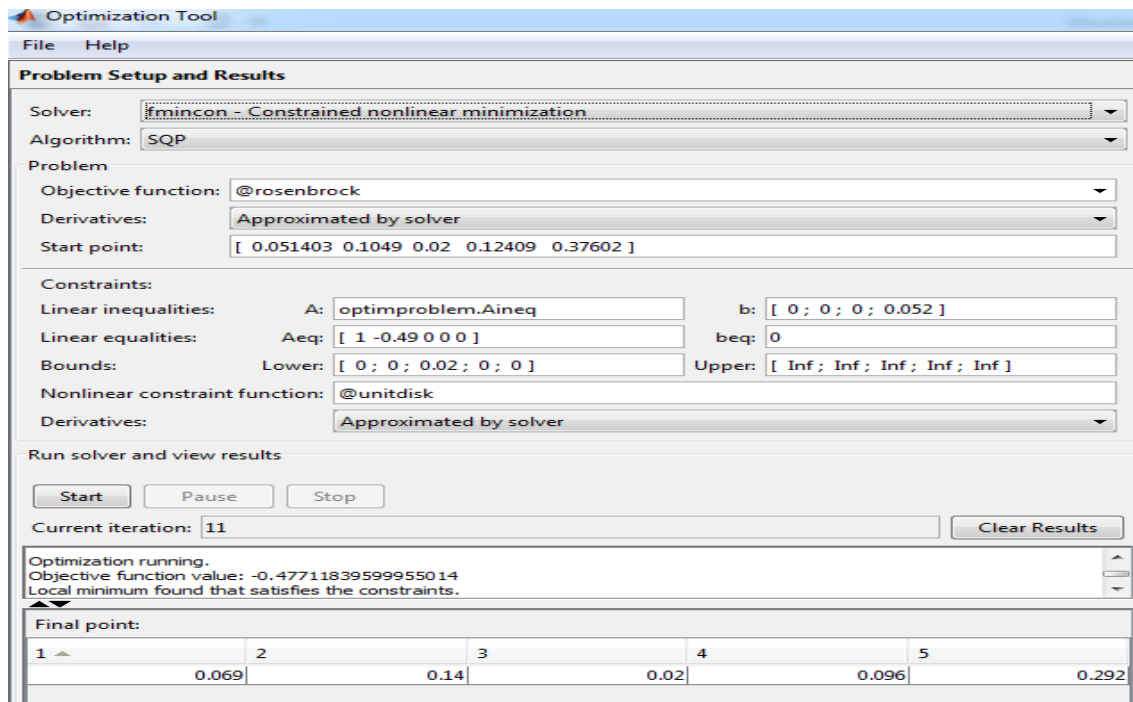

Figure 7-Optimization Toolbox using SQP algorithm

Figure-7 shows the optimization toolbox which was used to solve the optimization problem. The linear equality and inequality constraints were given as matrices. The Matlab files which were created for formulating the objective function and the nonlinear constraint equations are called in their respective fields in the toolbox. Once the bounds for the variables and the initial points for each variable is given, the optimization can be run. The order in which the values for bounds and initial points of the variables are given is [Ri,Ro,r,tw, H].

Optimization Results:

| Algorithm	No.of iterations	R_i (m)	R_o (m)	R (m)	tw (m)	H (m)	I_1 (kg.m2)
SQP	11	0.069	0.14	0.02	0.096	0.292	0.477
Active Set	5	0.069	0.14	0.02	0.096	0.292	0.477

Table 4-Opimization Results

Table- 4 shows the optimization results. At different initial points the same results were obtained thus indicating that the local minima obtained by solving this optimization problem is the global minima. Though the number of iterations vary according to the algorithm which is used to run the optimization, the results obtained were the same.

The optimization results give a Moment of inertia value of 0.477 kg.m2, the flywheel is optimized for its maximum possible angular velocity and minimum possible angular velocity. Thus by substituting the optimum moment of inertia value that is obtained after running the optimization, in the Kinetic energy equation, we get the maximum Kinetic energy stored in the flywheel to be 0.816 MJ. This is the total energy stored in the flywheel without considering the energy losses. The energy losses due to vibration, stator-rotor losses and the mechanical losses are calculated from the other subsystems, they are integrated with the structural subsystem and the net kinetic energy stored in the flywheel is calculated.

Optimization Plot Functions
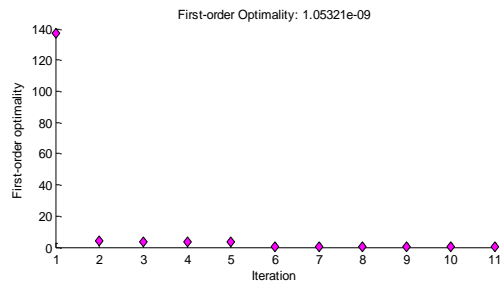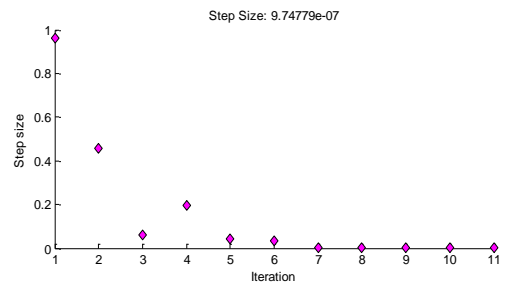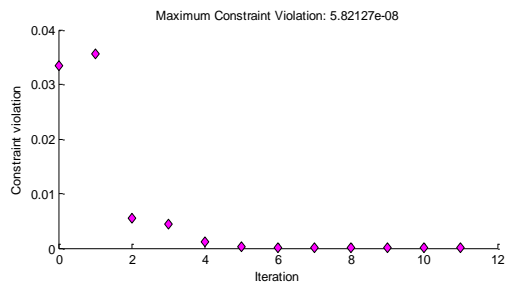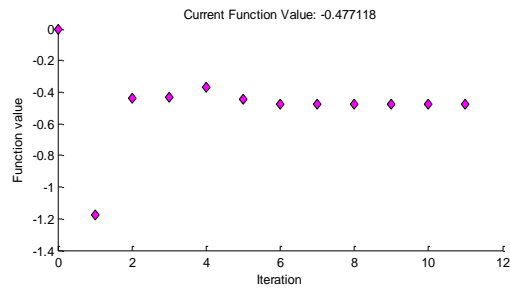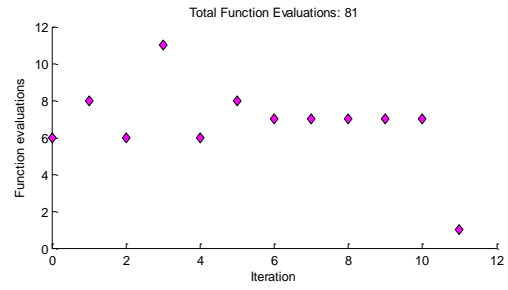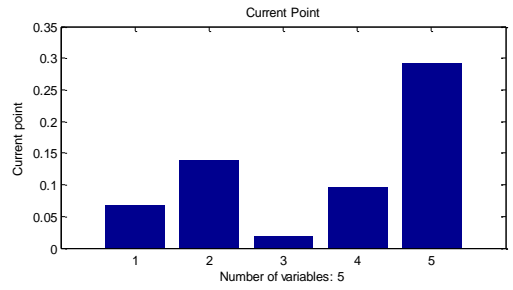
The optimization plot functions give details about the total function evaluations, optimal points, first order optimality and step size.

4.2 Optimal design of the coupling and flywheel for minimize the energy loss due to vibrations in coupling

4.2.1 Problem Statement

In Kinetic Energy Recovery Systems, the kinetic energy is usually transmitted from CVT to the flywheel through a mechanical coupling. Because of vibration in couplings, a huge amount of kinetic energy is being lost and it can't be delivered to the flywheel. This energy loss could be obtained from the equation 2.1.

$$\Delta.K.E = \left[\frac{1}{2}I_2\dot{\theta_2}^2(0)\right] - \left[\frac{1}{2}I_1\dot{\theta_1}^2(t) + \frac{1}{2}I_2\dot{\theta_2}^2(t)\right] \tag{2.1}$$

Where

I_1: Moment of inertia of the flywheel

I_2: Moment of inertia of the CVT's output shaft

$\dot{\theta_2}(0)$: CVT output disc's initial angular velocity at the time of engagement

$\dot{\theta_1}(t)$: Flywheel's angular velocity at desired time (t)

$\dot{\theta_2}(t)$: CVT output disc's angular velocity at desired time (t)

Because we are not going to design CVT system and by analyzing the equation (2.1) we can see that the first term in right hand side of the equation is constant. Because this term is constant, we are not able to optimize this term in order to minimize the energy loss. In order to minimize energy loss we should maximize second and third term in the right hand side of the equation. The second term is the kinetic energy stored in flywheel and the third term is kinetic energy stored in CVT after the desired period of time. Maximizing third term means we are maximizing energy stored in CVT which is a nonsensical optimization. So, for minimizing energy loss due to vibrations in coupling, we need to maximize energy stored in flywheel by optimal design of coupling and flywheel.
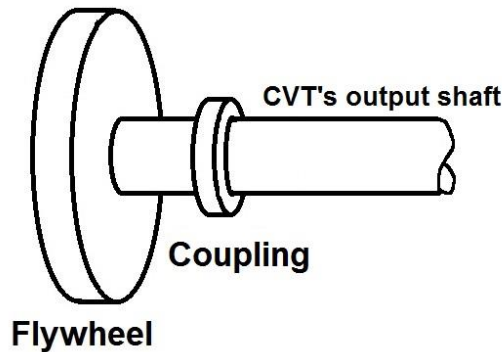

Figure 1: Schematic figure of CVT-Coupler-Flywheel system

4.2.2 Mathematical Model

4.2.2.1 Objective Function

In section 4.2.1 we described that in order to minimize the energy loss due to vibrations in coupling, we need to maximize the energy stored in the flywheel (equation 2.2).

$$\underset{max}{f} : \frac{1}{2} I_1 \dot{\theta}_1^2(t) \tag{2.2}$$

As you can see in the equation 2.2, there are two general variables I_1 and $\dot{\theta}_1$. I_1 is the moment of inertia of the flywheel. It includes several variables and parameters itself. We will talk about moment of inertia of the flywheel later section. $\dot{\theta}_1$ is the angular velocity of the flywheel that depends on the time. To calculate the angular velocity we need to find the equation of motion of the flywheel as a function of the time. This one also will be discussed in later section.

4.2.2.2 Constraints

This subsystem has totally seven variables: two of them are related to the coupling and going to be optimized in order to minimize the vibrations in the coupling. There are no constraints on these variables except that C and K both should be greater than zero.

Five of the variables are related to the flywheel and going to be optimized in order to maximize the energy is being stored in flywheel. There are six constraints for these variables. Some of these constraints are linear, some nonlinear. Some of them are equality and others are inequality constraints. In table 1 you could see all the constraints and their types.

Constraint	Type	equation
g_1	Geometric constraint	$R_o - R_i > 0$
g_2	Material strength	$\frac{3+\mu}{4} \rho \frac{v}{R_o} \left(R_o^2 + \frac{1-\mu}{3+\mu} r^2 \right) < S_y$
g_3	Geometric constraint	$t_w - 0.2H \geq 0$
g_4	Geometric constraint	$t_w - 0.4H \leq 0$
g_5	Volume constraint	$H\pi R_o^2 - 0.013 = 0$
g_6	Geometric constraint	$R_i - 0.49R_o = 0$

Table 1: Constraints

4.2.2.3 Variables and Parameters in tables

Tables 2 and 3 present all the variables and parameters have been used in both objective function and constraints in a nutshell. In the next section, we will describe how we got the values for these parameters.

Design variables	Symbol	Notations in codes	Unit
Thickness of the web	t_w	X(1)	m
Length of the flywheel	H	X(2)	m
Inner radius of the flywheel	R_i	X(3)	m
Outer radius of the flywheel	R_o	X(4)	m
Radius of the shaft	r	X(5)	m
Equivalent spring constant of the coupling	K	X(6)	$Kg.m^2/s$
Equivalent damping coefficient of the coupling	C	X(7)	$N.m/rad$

Table 2: List of variables

Design parameters	Symbol	Unit	Values and material used
Moment of inertia of the CVT	I_2	Kg/m^2	0.21 / steel 4330
Density of the material used for flywheel	ρ	Kg/m^3	2810 / Aluminum
Poisson's ratio of the material is used for flywheel	μ	--	0.3 / Aluminum
Yield strength of the material is used for flywheel	S_y	MPa	455 / Aluminum
Applied torque	τ	$N.m$	0 (At the time of engagement)

Table 3: Parameters used in objective function and constraints

4.2.3 Model Analysis

4.2.3.1 Decomposition of the objective function

As discussed, the objective function which we are going to maximize includes two general variables: I_1 and $\dot{\theta}_1$.

4.2.3.2 Decomposition of the moment of inertia of the flywheel

I_1 consists five variables and could be written as equation 2.4.

$$I_1 = I_s + I_r = \frac{1}{2}m(R_i^2 + r^2) + \frac{1}{2}m(R_o^2 + R_i^2) = \left(\frac{\rho\pi t_w}{2}\right)(r^4 - R_i^4) + \left(\frac{\rho\pi H}{2}\right)(R_i^4 - R_o^4) \qquad (2.3)$$

Where

t_w: Thickness of the web

H: Thickness of the flywheel

R_i: Inner radius of the flywheel

R_o: Outer radius of the flywheel

r: Inner radius of the rotor (outer radius of the flywheel's shaft)

We would label these variables x(1), x(2), x(3), x(4) and x(5) respectively.

4.2.3.3 Decomposition of the moment of inertia of the flywheel

To find the equation of the motion of the flywheel, we need to solve the coupled system of 2nd order ODEs shown in equations 2.4 and 2.5 at the same time

$$I_1\ddot{\theta}_1 + K(\theta_1 - \theta_2) + C(\dot{\theta}_1 - \dot{\theta}_2) = 0 \qquad (2.4)$$

$$I_2\ddot{\theta}_2 + K(\theta_2 - \theta_1) + C(\dot{\theta}_2 - \dot{\theta}_1) = \tau \qquad (2.5)$$

Where

I_1: Moment of inertia of the flywheel

I_2: Moment of inertia of the CVT's output shaft

$\ddot{\theta}_1$: Angular acceleration of the flywheel

$\ddot{\theta}_2$: Angular acceleration of the CVT's output shaft

$\dot{\theta}_1$: Angular velocity of the flywheel

$\dot{\theta}_2$: Angular velocity of the CVT's output shaft

θ_1: Angular position of the shaft

θ_2: Angular position of the CVT's output shaft

K: Equivalent torsional spring constant of the coupling

C: Equivalent torsional dashpot damping coefficient of the coupling

τ: Applied torque which is zero at the time of engagement

As you can see moment of inertia of the flywheel is again participating in equations of the motions. We will use the same notation as we used in 2.3 for calculating I_1.

Remember that we are going to minimize the kinetic energy loss due to vibrations in coupling. To do this, we need the find optimal values for the equivalent torsional dashpot damping coefficient of the coupling (C) and equivalent torsional spring constant of the coupling (K). At the same time, we must find the optimal dimensions of the flywheel in order to have the optimal design of the moment of inertia of the flywheel.

C and K are directly in equations 2.4 and 2.5. We will label them x(6) and x(7) when we want to build our script to solve the system of ODEs and pass the results to MATLAB *fmincon* toolbox.

Although there is an analytical solution for this system of 2nd order coupled ODEs, we would solve these equations numerically by writing a script using fourth-order Runge-Kutta method in MATLAB. The reason for solving this system numerically is that we are going to use MATLAB optimization tool box (*fmincon)* and in this case we are able to pass the numerical solutions of system of differential equations directly to MATLAB optimization tool. The process of solving this system of ODEs and implementing it in objective function in order to find the optimal values of *C* and *K* for minimum energy loss due to vibrations in coupling will be discussed in later section**.**

4.2.3.4 Finding parameters used in objective functions and constraints

In order to solve equations 2.3 and 2.4 and have completely known constraints, we need to find values for the parameters that participate in objective function and constraints.

One of the most important parameters that participates in equations 2.3 and 2.4 is moment of inertia of the CVT (I_2).

As we mentioned before, we are not going to design CVT so the moment of inertia of the CVT constant. CVT is a big and complicated transmission system that is connected to break system by its input shaft and to flywheel by its output shaft. Calculating moment of inertia is a really hard and tedious task and it is beyond the scope of this course. For the sake of simplicity, we are going to approximate the moment of inertia of the CVT by calculating the moment of inertia of secondary pulley set and planetary gear set mounted on output shaft.

The equation for computing I_2 is as follow:

$$I_2 = I_p + I_g \tag{2.6}$$

Where:

I_p: Moment of inertia of secondary pulley set

I_g: Moment of inertia of planetary gear set

$$I_p = \frac{1}{2} m_p r_p^2 \qquad (2.7)$$

$$I_g = \frac{1}{2} m_g r_g^2 \qquad (2.8)$$

By substituting $m = \rho V$ and $V = \left(\frac{\pi d^2 t}{4}\right)$ we have:

$$I_p = \frac{1}{2} \rho_p \pi t_p (r_p^4) \qquad (2.9)$$

$$I_g = \frac{1}{2} \rho_g \pi t_g (r_g^4) \qquad (2.10)$$

Where:

ρ_p: Density of secondary pulley set

ρ_g: Density of planetary gear set

t_p: Thickness of secondary pulley set

t_g: Thickness of planetary gear set

r_p: Radius of secondary pulley set

r_g: Radius of planetary gear set

Dimensions for conventional pulley and planetary gear set could be taken from technical papers. In table 4 you can see the dimensions used for this problem.

The secondary pulley set and planetary gear set are mostly made from steel 4330. From mechanical design handbooks density for this type of steel is 7850 kg/m^3.

	Secondary Pulley Set	Planetary Gear Set
Diameter(mm)	148.2	224
Thickness(mm)	44	100

Table 4: Dimensions of secondary pulley and planetary gear sets

Using data from table 1 and density of 7850 kg/m^3 for both pulley and gear set we have:

$I_2 = 0.21\ kg.m^2$

Other parameters which are either in equation 2.5 or in constraints are as follow:

v: Maximum allowable velocity at the tip of the flywheel (1000 m/s for this application)

ρ: Density of the material is used for flywheel (2810 kg/m^3 for aluminum)

μ: Poisson's ratio of the material is used for flywheel (0.3 for aluminum)

S_y: Yield strength of the material is used for flywheel (455 MPa for aluminum)

4.2.4 Optimization study and results
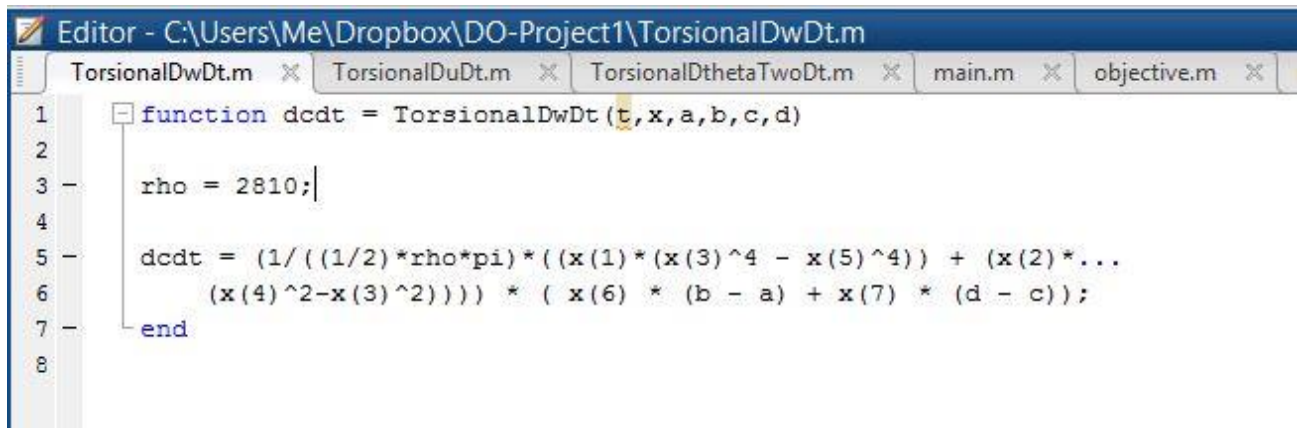
4.2.4.1 Finding equation of motion

As mentioned in previous section, to find equation of motion of the flywheel we are going to solve equations 2.4 and 2.5 by writing a script in MATLAB using 4th order Runge-Kutta method.

To solve a higher order ODE in MATLAB, we need to transform them to system of 1st order ODEs using change of variables method. Then we need to write four scripts for these two coupled ODEs. We also need four initial conditions in order to be able to solve the system. The initial angular position and velocity is zero for flywheel and angular position is also zero for CVT at the time of engagement but initial angular velocity of the CVT output shaft varies case by case. It actually depends on the speed of the vehicle when the driver hits the brake pedal and the output speed ratio of CVT. Based on different reviewed cases, the speed of CVT's output shaft at the time of engagement is between30000 to 65000 rpm in most cases. For this project, we take the lower bound as initial angular velocity of the CVT's output shaft.

The boundary conditions for this system are as follow:

1) $\theta_1(0) = 0$
2) $\theta_2(0) = 0$
3) $\dot{\theta}_1(0) = 0$
4) $\dot{\theta}_2(0) = 3140 (\text{rad/sec})$

Finally we should rewrite these equations based on our subsystem variables. In figures 2 you could see a screenshot of one of these scripts in MATLAB. The complete scripts for solving this system will be provided in appendices.


```matlab
Editor - C:\Users\Me\Dropbox\DO-Project1\TorsionalDwDt.m
TorsionalDwDt.m  ×  TorsionalDuDt.m  ×  TorsionalDthetaTwoDt.m  ×  main.m  ×  objective.m  ×
1    function dcdt = TorsionalDwDt(t,x,a,b,c,d)
2
3 -    rho = 2810;
4
5 -    dcdt = (1/((1/2)*rho*pi)*((x(1)*(x(3)^4 - x(5)^4)) + (x(2)*...
6           (x(4)^2-x(3)^2)))) * ( x(6) * (b - a) + x(7) * (d - c));
7 -  end
8
```

Figure 2 MATLAB script for solving

Next we should write a script based on Runge-Kutta method in order to solve this system. In figure 3 you would see a small part of this script as a snapshot.


```matlab
function [t,a,b,c,d]=Sys4ODEsRK4(ODE1,ODE2,ODE3,ODE4,A,B,h,a1,b1,c1,d1,x)
% Sys20DEsRK4 solves a system of two first-order initial value ODEs using
% fourth-order Runge-Kutta method.
% The independent variable is t, and the dependent variables are x and y.
% Input variables:
% ODE1 Name for the function that calculates da/dt.
% ODE2 Name for the function that calculates db/dt.
% ODE3 Name for the function that calculates dc/dt.
% ODE4 Name for the function that calculates dd/dt.
% x The first value of t.
% y The last value of t.
% h The size of a increment.
% a1 The initial value of a.
% b1 The initial value of b.
% c1 The initial value of c.
```

Figure 3: Script written for the 4th order Runge-Kutta algorithm

After writing these scripts which are related to solving equations 2.4 and 2.5 numerically, we need to write some scripts for finding the optimal values for subsystem's variables. The first script is for nonlinear constrains, either equality or inequality ones. You can see the screenshot for this code in figure 4.


```matlab
function [g , h] = nonlincond(x)

Sy = 455e6;
Mu = 0.33;
rho = 2810;
v = 1000;

% Tw = x(1);
% H = x(2);
% Ri = x(3);
% Ro = x(4);
% r = x(5);

g = ((3+Mu)/4)*rho*((v/x(4))^2)*(x(4)^2*+((1-Mu)/(3+Mu))*x(5)^2) - Sy;
h = x(2)*(x(4)^2)-0.0041;
end
```

Figure 4: Script for nonlinear constraints

There is one more script that we need to write which is for objective function (equation 2.2). To write objective function we need to have the angular velocity of the flywheel at

22

the desired time. The usual time period of engagement of flywheel and CVT is 6.67 *sec* based on technical papers. By putting 6.67 *sec* as our desired time and get the corresponding value for the angular velocity of the flywheel and pass it to objective function, we can make the objective function ready in order to use it for optimization tool. In figure 5 you could see the screenshot of the code has been written for the objective function.

```matlab
function f = objective(x)

rho = 2810;

% Tw = x(1);
% H  = x(2);
% Ri = x(3);
% Ro = x(4);
% r  = x(5);
% K  = x(6);
% C  = x(7);

[t,a,b,c,d] = Sys4ODEsRK4(@TorsionalDthetaOneDt,...
    @TorsionalDthetaTwoDt,@TorsionalDwDt, @TorsionalDuDt,...
    0,6.67,0.1,0,0,0,3140,x);
theta1dot = c(end);
f = -((1/2)*((1/2)*rho*pi)*((x(1)*(x(3)^4 - x(5)^4)) + (x(2)*...
    (x(4)^4-x(3)^4))) * theta1dot^2);

end
```

Figure 5: Script for objective function (total time of engagement, initial speed as and final objective function in red, green and yellow boxes respectively)

Finally to get the optimal values we would use MATLAB's optimization tool called *fmincon*. For our purpose, there are three different algorithms implemented in it. These algorithms are: interior points, SQP and active set. We are going to use all of them for our subsystem and see the results.

Although we start with initial guesses that are close enough to the actual values of a real model, we will get the same answers with changing the initial points while we are using the same optimization algorithm. In table 5 you can see the values for the initial guess that we took.

	t_w	H	R_i	R_o	r	K	C
Initial Guess	0.04	0.04	0.08	0.1	0.03	170	0.45

Table 5: Initial guess used in optimization tool

The only difference between final answers happens when we try different algorithms in *fmincon* toolbox. The optimal results for the Interior Points and Active Set algorithms is somehow the same. For these two algorithms the number of iterations only changes. The optimal values for the SQP algorithm shows almost big differences for the inner and outer radius of the flywheel. In table 6 you can see the optimal results by applying different algorithms.

	Iterations	t_w	H	R_i	R_o	r	K	C
Interior Points	73	0.046	0.144	0.098	0.199	0.03	170. 1	**0.834**
Active Set	4	0.052	0.136	0.1	0.205	0.03	170	**0.45**
SQP	7	0.066	0.225	0.078	0.159	0.03	170	**0.45**

Table 6: Optimal results for three different optimization algorithms

4.2.5 Discussion of the results

4.2.5.1 Search for the global solutions

As discussed in previous section, b trying different initial guesses we got the same optimal results for our subsystem. That means we have found our global solution for this problem.

By comparing our final results for *C* and *K* we would see that these values are really close to the actual equivalent values for a coupling is used in a Kinetic Energy Recovery System (KERS). From technical papers, those couplings that are being used in KERS usually have the equivalent spring constant about *200 N.m/rad* and equivalent damping coefficient of *0.6 Kg.m²/s*.

The same thing is also true for the optimal values of the flywheel's dimensions.

4.2.5.2 Physical interpretation of the results

If we implement the optimal results taken from optimization tool and substituting them in the scripts written for solving system of ODEs and writing a new script to plot the angular velocity of the flywheel and CVT during the period of the engagement (6.67 second), we will have the figure 6 as the result.
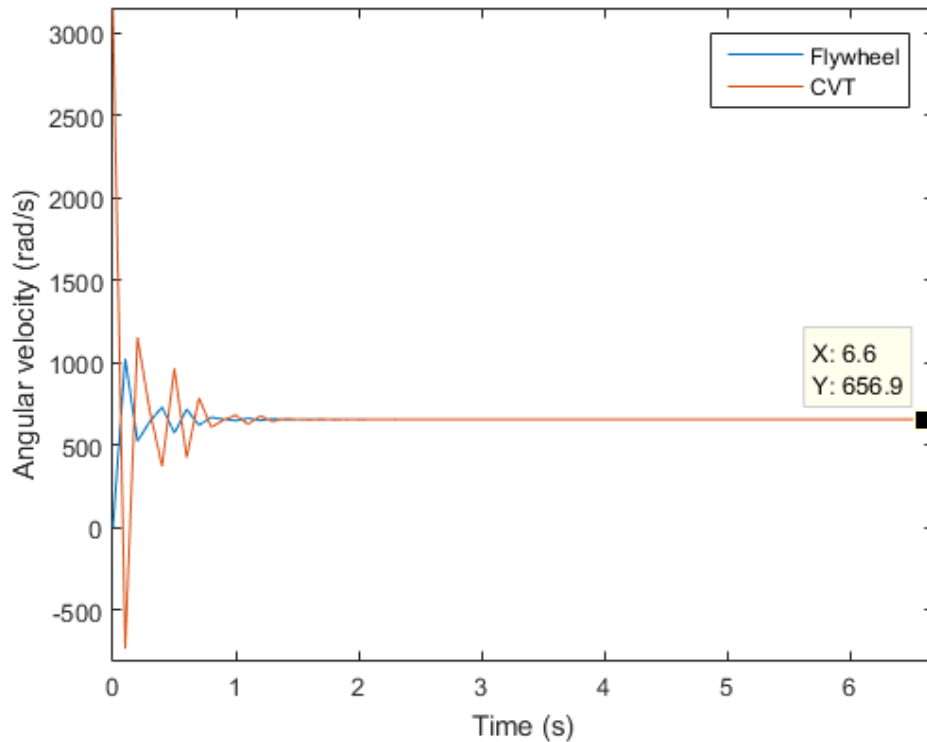
Figure 6: Angular velocity of the flywheel and CVT based on optimal results

As you see in figure above, the CVT starts from initial speed (*3140 rad/s*) and flywheel starts from speed zero. Then due to vibrations in coupling the velocity of CVT decreases and velocity of flywheel increases. Because the equivalent damping coefficient of the coupling is relatively high, the system goes to the steady state after only 1.5 seconds and vibrations in the coupling disappears. From this time to the end of the engagement both flywheel and CVT rotates with the same angular velocity of 657 rad/sec.

One could argue that because there is a huge drop in angular velocity of the system, these *C* and *K* values. As we described in sections 2.1 and 2.3, we were trying to minimize the energy loss in the coupling with respect to maximize storable energy in flywheel. To make that happen, the system should go to the steady state very soon. The point is that if C is low and K is very high, the system would oscillate for a long period of time. In this case it might possible that the energy loss from coupling be lower but the point is that most of this energy will be still in CVT. This argument could be better grasped by bringing another figure for angular velocity when the flywheel has the same dimensions but the value of *K* is greater than and the value of the *C* is lower than the optimal value.
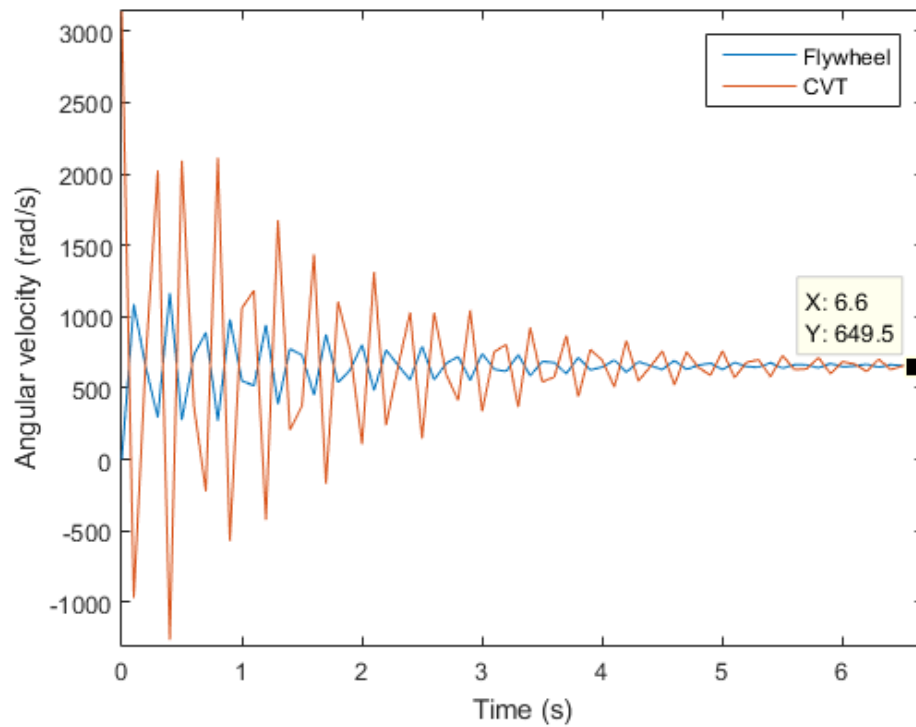
Figure 7: Angular velocity of the flywheel and CVT based on changing the values of C and K

As you can see in this figure, with changing *K* from 170 to 185 and C from 0.83 to 0.6, angular velocity of the flywheel is 650 *rad/s* which is less than the angular velocity for previous figure. It means than the energy that stored in flywheel is less than previous state.

4.3 Design optimization of a flywheel system by minimizing the losses in the magnetic bearings

4.3.1 Introduction

Flywheels are increasingly used as a means for energy storage; thanks to their capacity to store an important quantity of energy, their long lifetime and their large charge/discharge cycles. To store a large amount of energy, high speed composite materials are often used and the flywheels are run at very high speeds. Due to their high speed operation, contactless bearings are required in order to reduce the friction losses which are important in the flywheel applications. Thanks to the absence of contact between rotating and non-rotating parts of a system, magnetic bearings system is used such high speed rotating systems. When the motor speed is 96000 RPM, frequency can reach up to 1600 Hz. The loss generated by the high frequency stator current and the high frequency core magnetic flux are far greater than that at low frequencies, therefore the rising temperature and noise generated by the high loss will produce great impact on the motor performance. So reducing the motor loss and improving the efficiency are the primary objectives in these systems. Motor loss is closely related to the electromagnetic field distribution inside the motor, and the flux distribution inside the motor is closely related to the motor generic dimensions. Therefore, for optimal efficiency, analysis of the critical dimensions of the stator and the rotor is essential.

4.3.2 Problem Statement

As mentioned earlier, high speed rotating systems use magnetic bearings to reduce the contact forces between the rotating and non-rotating parts. This work deals with various losses in this magnetic bearing system and to be more specific, it deals with minimizing the losses in the magnetic stator rotor system. But while doing so we need to keep in mind the design constraints of the flywheel system, both its geometric restrictions as well as the strength criteria. Hence we need to find a way to satisfy all the requirements while minimizing the losses. So the objective is to minimize these losses while finding the optimal design of the flywheel system.

4.3.3 Mathematical Model

The most notable losses in the system are the stator iron loss, stator copper loss, rotor eddy current loss and the rotor windage loss. The following sections briefly describes each loss. We will also see the effect of each of these losses on the split and aspect ratios.

4.3.3.1 Stator Iron Loss

Stator Iron loss (also called as stator core loss) is further divided into the hysteresis loss and the eddy current loss. These core losses depend on the frequency of the stator. Eddy current losses are minimized by lamination of the core. If the flux density is sinusoidal, the stator iron loss is given by the following equation.

$$P_{fe} = K_h f B_m^a + K_{el} f B_m \qquad \text{(i)}$$

where, f is the frequency of the magnetic flux wave form, B_m is the peak of the sinusoidal flux density, 'a' is the Steinmetz constant, K_h is the hysteresis constant, K_{el} is the eddy current constant.
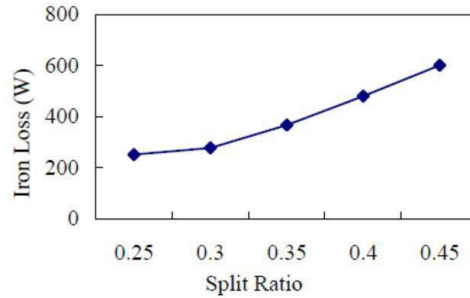
Figure 8 Iron loss vs Split Ratio

4.3.3.2 Stator Copper Loss

Copper loss forms a major proportion in the loss in the magnetic bearings. This loss is attributed to the electrical resistance in the stator winding. Hence this loss is often termed as winding loss.
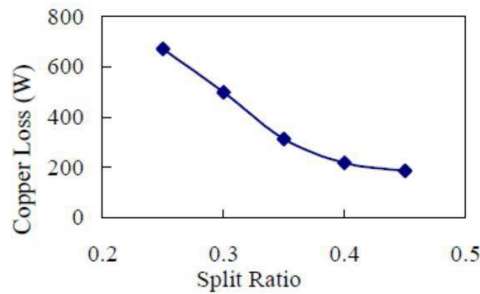
Figure 9 Copper Loss vs Split Ratio

4.3.3.3 Rotor eddy current loss

Cogging of the stator will produce non-sinusoidal stator magneto motive force (MMF), while the distribution of winding current is non-sinusoidal, that will produce flux density including space harmonic and time harmonic. Air-gap flux density harmonics will generate eddy current losses in the rotor conductor.
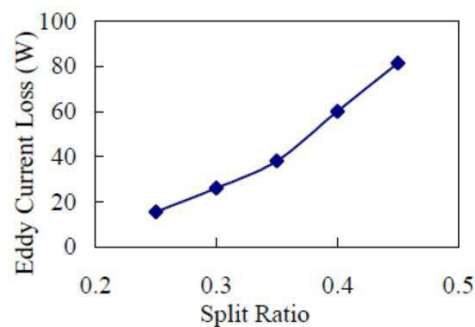
Figure 10 Eddy Current loss vs Split Ratio

4.3.3.4 Rotor Windage Loss

Due to the high rotor speed, rotor windage loss is so larger that it needs to be considered. Different exposure forms friction losses on the surface and end of rotor are different. Different split ratio will affect both surface windage loss and the end windage loss. Overall effect of split ratio on the windage loss is shown in the following graph.
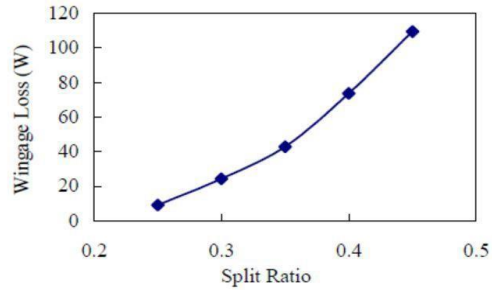
Figure 11 Windage loss vs split ratio

4.3.3.5 Variation of total loss vs split ratio

As we can see from the above graphs, all the losses behave differently with the change in the split ratio. It becomes interesting to note the effect of the split ratio on all the losses considered together. This effect is given by the following graph. We can successfully derive an equation of the graph shown above.
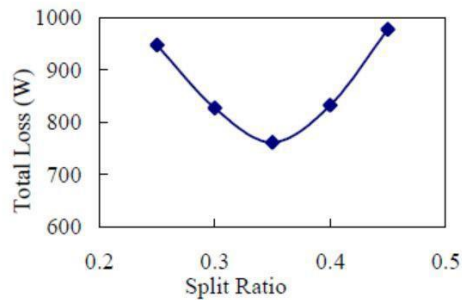
Figure 12 Total loss vs Split ratio

The curve fitting tool of MATLAB does the job for us. This equation is very use full and forms a part of the objective function for us. The equation is given below.

$$L_1 = 33330x_1^4 - 3333x_1^3 + 916.7x_1^2 - 5342x_1 + 2150$$

(ii)

4.3.3.6 Variation of total loss vs Aspect ratio

A similar analysis is performed but by varying the aspect ratio of the rotor this time. The final graph of the total loss with respect to the aspect ratio is given below.
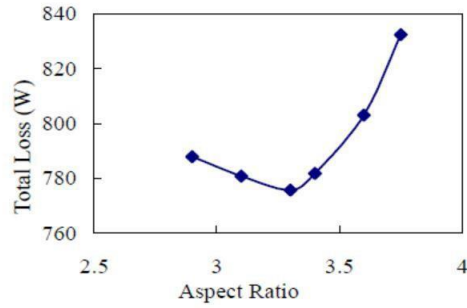
Figure 13 Total loss vs Aspect ratio

The equation for which is obtained from MATLAB and is given as

$$L_2 = -8.937x_2^4 + 260.2x_2^3 - 1829x_2^2 + 4872x_2 - 3672 \qquad \text{(iii)}$$

Various formulations for the design optimization problem of the flywheel rotor have been published. One of those dealing with geometric parameters reads as

Min $f(x) = f(L_1, L_2)$
Subject to geometric constraints $\qquad \text{(iv)}$

This is a multi-objective problem and many methodologies have been proposed by various researchers over the years to solve such optimization problems. In this project we consider the first function as the objective function and introduce the second function as an inequality constraint. This will be explained in detail in the further sections.

4.3.3.7 Design Variables and Parameters

The various design variables and parameters (other than the rotational speed) which will be used here are mentioned in Table 1. All those mentioned in the table but tg are design variables. Many design variables directly influence the flywheel setup. For example, it was shown in Ha, Yang and Kim (1999) that a lay-up with radially increasing hoop stiffness to density ratio is the most beneficial in terms of energy capacity. The rotational speed is also a common quantity that influences the specific kinetic energy stored. Thus, there exists a critical rotational speed for any type of rotor. However, the rotational speed is different from the commonly discussed design variables in that it varies with service conditions. Hence it is often considered as a parameter. The below table lists some of the quantities.

Quantity	Variable
Split Ratio	x_1
Aspect Ratio	x_2
Rotor Length (L)	x_3
Shaft diameter (2r)	x_4
Stator outer diameter (d_{so})	x_5
Flywheel inner radius (R_i)	x_6

30

Web Thickness (t_w)	x_7
Flywheel outer radius (R_o)	x_8
Flywheel Length (H)	x_9

Table 1 Design Variables

4.3.3.8 Constraints

The design problem stated in Eq. (4) is constrained by the strength limits of the structure, geometrical bounds and dynamical considerations. In this work we consider the geometric constraints. Geometrical bounds arise from the design of the surrounding components. A given shaft, hub or casing geometry can restrict the dimensions of the rotor, i.e. the inner and outer radii as well as the axial height. The aspect ratio and the absolute size in conjunction with the bearing properties can also necessitate size constraints in terms of dynamic stability for large rotational speeds. Similarly the whole flywheel system is constrained by the volumetric limits. The following are some of the geometric constraints that can be considered

$$0.5x_4 - x_6 + x_7 = 0 \qquad \text{(v)}$$

$$\frac{x_3}{2x_2} - 0.5x_1x_5 + 0.0024 = 0 \qquad \text{(vi)}$$

$$\frac{x_6}{x_8} - 0.49 = 0 \qquad \text{(vii)}$$

$$x_8^2x_9 - 0.0057325 = 0$$
$$\text{(viii)}$$

$$0.5x_4 - x_5 \leq 0$$
$$\text{(ix)}$$

$$0.5x_5 - x_6 + 0.0025 \leq 0 \qquad \text{(x)}$$

$$x_3 - 0.5x_9 + 0.00025 \leq 0 \qquad \text{(xi)}$$

$$8.937x_2^4 - 260.2x_2^3 + 1829x_2^2 - 4872x_2 + 4432 \leq 0$$
$$\text{(xii)}$$

$$(x_1 - 1)x_5 \leq 0$$
$$\text{(xiii)}$$

$$0.002 - \frac{x_3}{x_2} - x_1x_5 \leq 0 \qquad \text{(xiv)}$$

$$x_4 - \frac{x_3}{x_2} + 0.005 \leq 0 \qquad \text{(xv)}$$
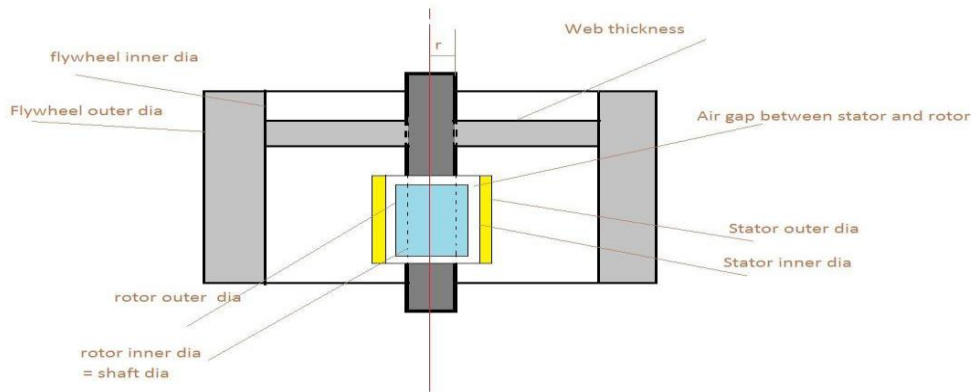
Figure 14 Flywheel system

The following table gives the lower and upper bounds on the variables being considered in this problem. All these constraint equations and the bounds on the variables are derived from the geometric requirements of the design. Equation (viii) is a result of the volumetric constraint. Equation (xii) is obtained from equation (iii), where we rewrote the equation (iii) as an inequality constraint. The logic behind equation (xii) from equation (iii) goes as follows. When we consider only the equation (iii) and minimize it, we get the minimum value as 760W. But now we have to consider minimizing equation (ii) along with equation (iii). This can be done by minimizing equation (ii) while compromising on the minimum value of equation (iii) to some level such that the optimum is reached and system performance is maximized.

Variable	Lower Bound	Upper Bound
x_1	0	1
x_2	1	Inf
x_3	0	inf
x_4	0.05	Inf
x_5	0	Inf
x_6	0	Inf
x_7	0	Inf
x_8	0	0.25
x_9	0	Inf

Table 2 Lower and upper bounds on variables

4.3.4   Model analysis

Before sending the problem into the optimizer, it is necessary to conduct some initial study on the objective function and constraints. Monotonicity analysis could be employed to help determine if the problem is well bounded and determine active constraints.

	x_1	x_2	x_3	x_4	x_5	x_6	x_7	x_8	x_9
F	+	.	.	.	.	.	.	.	.
g1	.	.	.	.	+	-	.	.	.

g2	.	.	+	.	.	.	.	.	-
g3	.	-	.	.	.	.	.	.	.
g4	+	.	.	.	-	.	.	.	.
g5	-	+	-	.	-	.	.	.	.
g6	.	+	-	+	.	.	.	.	.

Table 3 Monotonicity table

4.3.5 Optimization study

We now have the objective function, various constraint equations and the lower and upper bounds on the variables. All we need to do is to optimize the problem. The optimization has been carried out with the aid of MATLAB optimization toolbox. Optimization Toolbox provides functions for finding parameters that minimize or maximize objectives while satisfying constraints. The toolbox includes solvers for linear programming, mixed- integer linear programming, quadratic programming, nonlinear optimization, and nonlinear least squares.

4.3.5.1 Function formulation in MATLAB

We create a rosenbrock file and enter the objective function as shown in the following figure 8. Rosenbrock is generally used for nonlinear functions.

Figure 15 Rosenbrock function script in MATLAB

4.3.5.2 Constraints function in MATLAB

We create a function for the constraint equations. This is shown in figure 9 below.

Figure 16 Nonlinear constraint script in MATLAB

4.3.5.3 Optimization app

- We start the app using the command optimtool
- Select fmincon as the solver.
- Select SQP from the algorithm.

- Call the objective function by typing '@rosenbrock' in the field.
- Enter the initial values for the variables.
- Enter the linear inequalities, equalities and give the lower and upper bounds for the variables.
- Call the nonlinear function by typing '@unitdisk' in the field.
- In the right half pane, select the required plots, modify the iteration tolerance values, Hessian etc. as required.
- Start the optimization.

4.3.5.4 Results

The following table shows the optimal values of the variables obtained in the optimization process.

variable	Quantity	Optimal Value (SI system)
x1	Split Ratio	0.355
x2	Aspect Ratio	2.222
x3	Rotor Length	0.116
x4	Shaft diameter	0.05
x5	Stator outer diameter	0.154
x6	Flywheel inner radius	0.08
x7	Web Thickness	0.055
x8	Flywheel outer radius	0.166
x9	Flywheel Length	0.232
Fmin	Minimum function value	753.64

Table 4 Optimal Values of the design variables
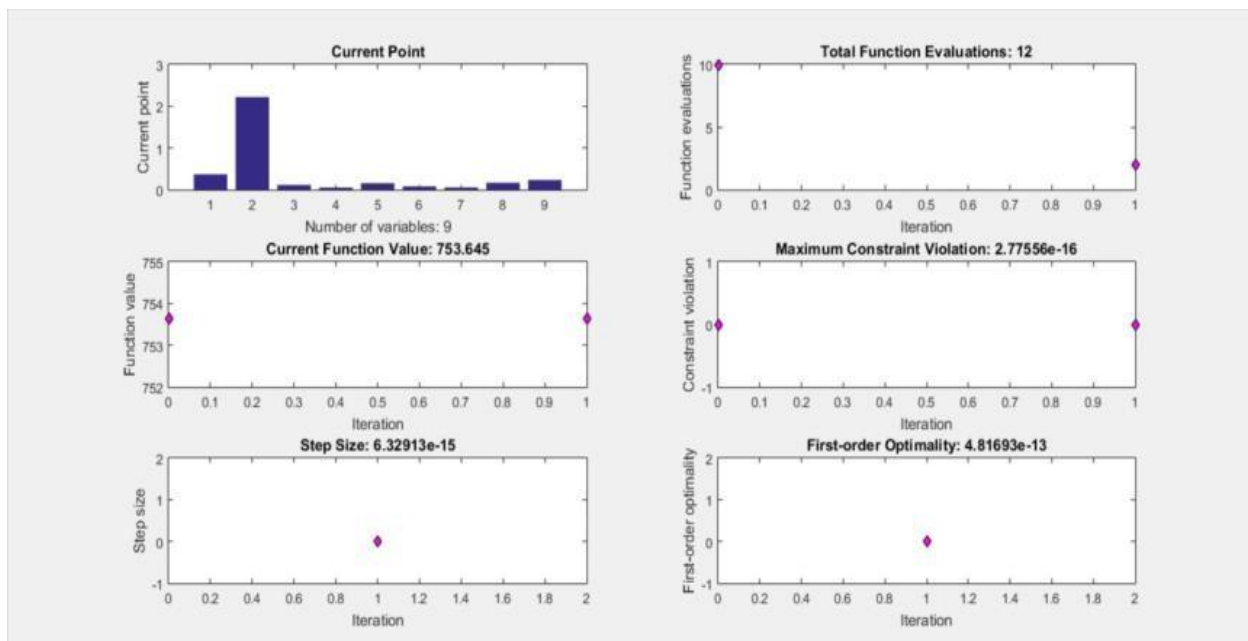
Figure 17 Optimization plots

The above figure contains the details of the optimal points, Number of function evaluations required and the optimal function value.

As mentioned earlier, split ratio is the ratio of the stator inner diameter to the stator outer diameter. The aspect ratio is the ratio of the rotor length to the rotor outer dia. It can be observed from the above results that the shaft diameter is hitting the lower bound. This is because of the face that no other constraint is active except the lower bound. To mention again, we have stated earlier that we will be considering only the geometric constraints in this subsystem. Had we used the strength constraint on the flywheel and the shaft, we would have got a value for the shaft diameter which can support the flywheel vibrations and its weight. But that part is left for the other subsystems. So just a minimum value on the shaft diameter has been considered here.

Similarly, if we observe, we have given an upper bound for the outer radius of the flywheel. The reason for this is that when we gave the volume constraint, it can change both length of the flywheel or the outer radius of the flywheel. From our analysis, we found out that if the upper limit on the flywheel outer radius had not been given, then we get a very large flywheel outer radius value and a very small length of the flywheel value. But these are not consistent with the practical systems. Hence the upper bound on the outer radius has been given.

Further these results do not give the global optimum values. The reason is that most of geometric constraints we used are in terms of ratios. So for different initial points we can have different optimal values which satisfy the constraint equations. Hence we give the volume constraint and give the initial points accordingly.

4.4 Optimization of a flywheel system by minimizing the mechanical losses

4.4.1 Introduction

The efficiency of flywheel depends mainly on the capacity to store maximum energy. Though our overall objective function will be to maximize the energy stored, maximizing of kinetic energy stored can be viewed from a point where we have to reduce the losses leading to improved storage of kinetic energy. The major losses in the system is due to the frictional and aerodynamic drag force. The other major loss is due to clutch slipping

$$\text{Total } KE_{veh} = \text{Total } KE_{fly} + E_{loss \ (friction+aero)} + E_{loss \ (clutch)}$$

This project focuses mainly on the flywheel design optimization hence we will be concentrating on the drag losses in the flywheel and stator.
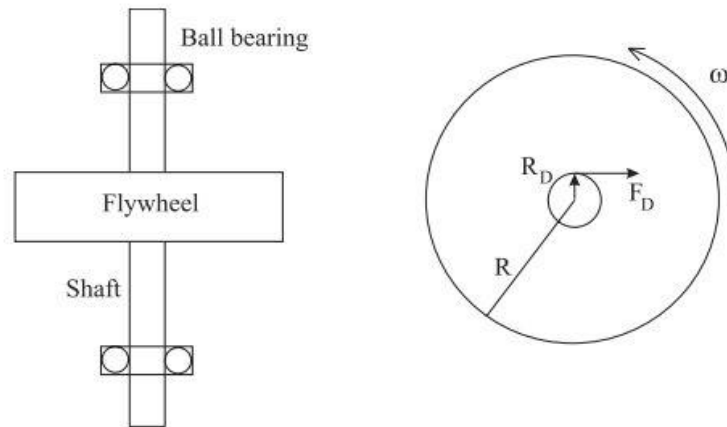
Figure: shows a simple sketch of flywheel along with the drag force in bearing

The two important losses that this subsystem will be dealing will the aerodynamic drag force on the surface of flywheel and air frictional losses inside the rotor stator system.

4.4.2 Design Problem Statement

The main design problem here is obtain an optimal point for which the power loss is minimal and the values are in feasible range agreeing with the constraints. Thus our main objective for this subsystem would be to minimize the energy lost due to drag effect and also frictional losses between the web and surrounding air.

4.4.3   Mathematical Model

The mathematical model gives a brief insight of the variables, objective and constraints of this system

4.4.3.1 Design Variable

Variables	Description	Units
R_o	Outer radius of flywheel	Meter
R_i	Inner radius of flywheel	Meter
H	Length of flywheel	Meter
r	Radius of shaft	Meter
d	Distance from web to top of flywheel	Meter

4.4.3.2 Intermediate parameter

Variables	Description	Units
C_d	Coefficient of drag	
R_e	Reynold's Number	
C_f	Friction coefficient	
K_f	Shape function	

4.4.3.3 Material Constants

Variables	Description	Units
ρ_a	Density of air	Kg/m^3
ω	Angular velocity	Rpm
ϑ	Dynamic viscosity	Kg/m-s
π	Pi constant	

4.4.3.4 Objective function

a.   Aerodynamic drag losses in the flywheel system

The most notable losses in the system are the aerodynamic drag losses on the surface of flywheel due to high speed of rotation.

Flywheel is a simple device which stores torque coupled to a large moment of Inertia. The governing equation is simple

$T = I\omega + T_d$

where T is shaft torque, T_d is the aerodynamic drag toque, I is the rotational moment of Inertia and ω denotes the time derivative of angular velocity. The total amount of kinetic energy stored in the rotating mass is

E=½ Iω²

The aerodynamic drag of spinning flywheel is estimated by considering the shear drag on a flat plate, aligned parallel to a fluid stream

F_{plate} = ½ C_{df} ρAV²

where F_{plate} is the drag force, C_{df} is the shear drag coefficient, ρ is fluid density A is area under contact and V is linear velocity. The flywheel is cylindrical with thickness D, we can integrate equation over the entire surface of the flywheel, and deduce the total drag torque:

$$T_d = \iint_S F_{plate}\, r dA = \pi \rho C_{Df} \omega^2 \left(\tfrac{2}{5} r^5 + Dr^4 \right)$$

where r is outer radius of flywheel and D is length of flywheel

$$P_{drag} = \rho_a \pi\, C_{df}\, \omega^3 \left(\tfrac{2}{5} R_o^5 - H R_o^4 \right)$$

where R_o is outer radius of flywheel and H is length of flywheel

A number of empirical formulas exist to determine the drag coefficient and in this case the following formula for turbulent flow is used (from Munson et al. (1990)):

$$C_{Df} = \frac{0.455}{(\log(Re))^{2.58}}$$

where the Reynolds number R_e is based on the flywheel radius and tip speed

$$Re = \left[\frac{\rho_a\, \omega\, R_o^2}{\vartheta} \right]$$

b.   Air frictional losses in web of flywheel

The 'I' shaped web connecting the flywheel and the shaft creates air friction when rotating at high speed. An estimation of the loss can be made by approximating the geometry of the rotating part of the web as a disc.
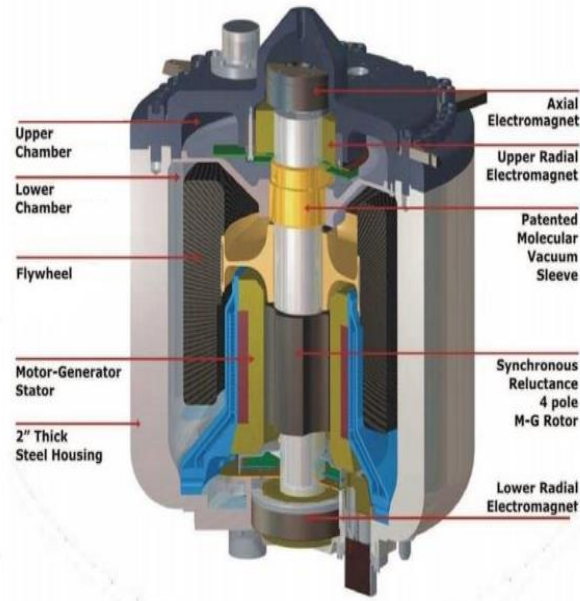
Figure: A cut section view of flywheel energy storage system

The disc is enclosed in its own cylindrical container. The quota between the axial distance from the disc to the enclosure, and the outer radius of the disc determines the topology of the flow inside the machine. This quota is called the spacing ratio
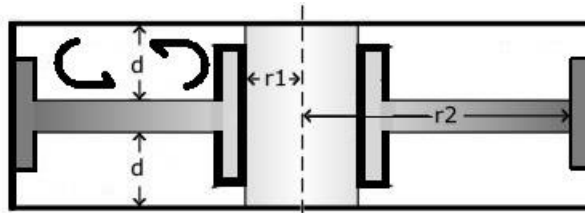
Figure: Schematic picture of a disc rotating inside a cylindrical enclosure.

The arrows describe the radial mass transport occurring in the turbulent flow regimes. Of particular interest is the ratio d/r_2, called the spacing ratio. The power loss experienced by a disc inside a cylindrical enclosure can be written as

$$P_{air} = \frac{\left(K_f \rho_a \, C_f \, \omega^3 \left(R_i^5 - r^5\right)\right)}{2}$$

where M_{disc} is the friction torque on the surface of a smooth, thin rotating disc and k_f a dimensionless roughness factor (1 for a completely smooth disc).

The friction torque on a rotating disc can further be calculated by the equation:

$$M_{disc} = \frac{C_f \rho_a \omega_m^2 \left(r_o^5 - r_i^5\right)}{2}$$

where ρ_a is the density of air, ri and ro the inner and outer radii of the disc respectively, and C_f the friction coefficient. The friction coefficient depends to a large extent on the flow pattern generated between the web and the enclosure. A summary of the equations governing the friction coefficient in each of these regions can be found in Table

Regime	Description	C_f (best empirical)
I	Laminar flow, small gap; Merged boundary layers	$C_f = \dfrac{2\pi}{(d/r_2)R_e}$
II	Laminar flow, large gap; Separate boundary layers with constant velocity core	$C_f = \dfrac{3.70(d/r_2)^{1/10}}{R_e^{1/2}}$
III	Turbulent flow, small gap; Merged boundary layers, radial mass transport	$C_f = \dfrac{0.08}{(d/r_2)^{1/6} R_e^{1/4}}$
IV	Turbulent flow, large gap; Separate boundary layers with radial mass transport No radial mass transport in core	$C_f = \dfrac{0.102(d/r_2)^{1/10}}{R_e^{1/5}}$

where Re is the so called tip Reynolds number, the Reynolds number of a disk rotating in free space, defined as:

$$R_e = \frac{\rho_a \omega_m r_o^2}{\mu},$$

and μ is the dynamic viscosity of air.

Regime I and III are characterized by a small air gap between the rotating and static surface. The small air gap makes it possible to approximate the flow between the rotating and static surfaces as homogenous, either laminar or turbulent. For the large gaps, separate boundary layers are formed (regime II and IV). Between the layers, there is a core with approximately constant velocity. The laminar boundary layers of region II turn turbulent at higher rotational velocities, i.e., Reynolds numbers.

4.4.3.5 Constraints

a. The difference between the inner radius and outer radius of flywheel must be always strictly greater than zero.

$$g1: R_o - R_i > 0$$

The flywheel cannot be a solid on as there is motor and generator attached to lower half of the shaft of flywheel and bearing attached to top of the flywheel.

b. The stress constraint is one of the critical constraint which relates the Outer radius of the flywheel to inner radius of the shaft which is given as follows

$$g2: \frac{3+\mu}{4}\rho\omega\left(R_o^2 + \frac{1-\mu}{3+\mu}r^2\right) \leq S_y 0$$

The explanation for the stress criteria has already been given in the first section.

c. The distance of d is taken in a range from the literature which varies from about 1/3 to 1/4 of length of the shaft.

$$g3 : d - 0.25H \geq 0$$
$$g4 : d - 0.33H \leq 0$$

d. The volume of the enclosed container is taken as constant. The volume is total space occupied by the flywheel hence it gives a relation between outer radius of flywheel and height of the shaft.

$$g5 : H\pi R_o^2 = Volume$$

e. The radius ratio is a very important constraint obtained from literature. It gives a relation between inner and outer radius of the shaft. This is obtained for maximum possible specific energy and energy density as explained in the first subsystem.

$$g6 : R_i/R_o = Constant$$

f. The inner radius of the

$$g7 : R_i - r > 0$$

The greater than constraints have been converted to negative null form to be used in the optimization toolbox. In case of strictly greater than equation, it was converted to negative null form with some constant value on the right side of the equation.

4.4.4   Model Analysis

4.4.4.1 Pre-optimization visualization of influence of variables on the power loss due to drag

The variables that influences the drag force that occur in flywheel are Ro and H of the flywheel. Before, optimizing them for getting minimal loss in flywheel due to drag forces it is necessary to conduct some initial study on the objective function and their effect on variables. Thus a contour plot and XY plot was done to get a better understanding on the influence of these variables on the total drag loss

A simple plot of variation of outer radius for different values of H (length of flywheel) was plotted. This plot shows the nonlinear relation of outer radius with respect to drag force, it presents an idea of the great magnitude at which the flywheel drag manifests after about 0.15 m. It also shows the influence of H is higher in high radius values compared to smaller outer radius.
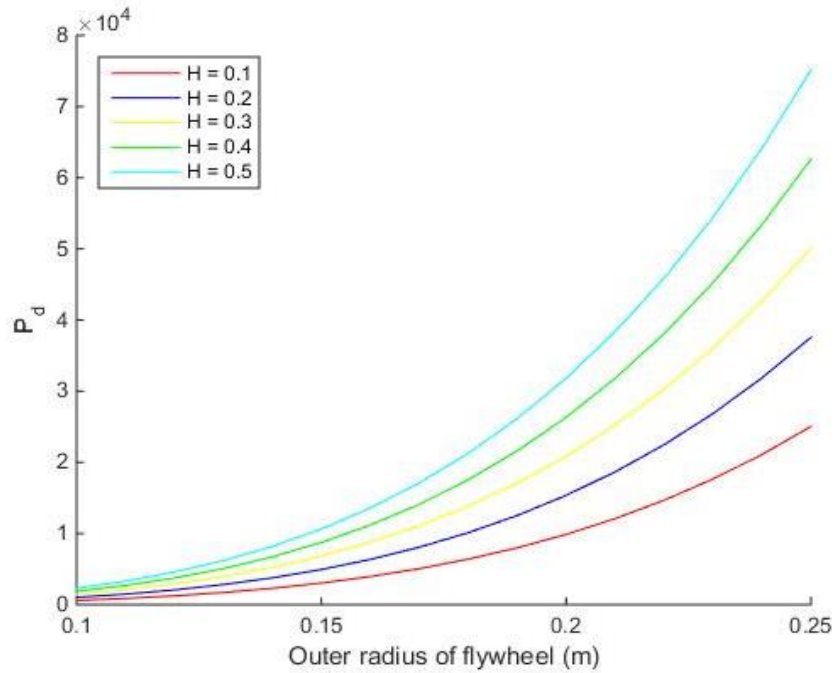
Figure: Plot showing variation of value of Pdrag with respect to R_o for a constant H

The Contour plot of power loss due to drag with respect to outer radius and height gives us more holistic view on the effect. This shows a better range of values for our optimization range. It can be observed that if outer radius is lesser than 0.25 m it is in range of least value for the whole range of height of flywheel, so we understand that a constraint is required to restrict these two variables.
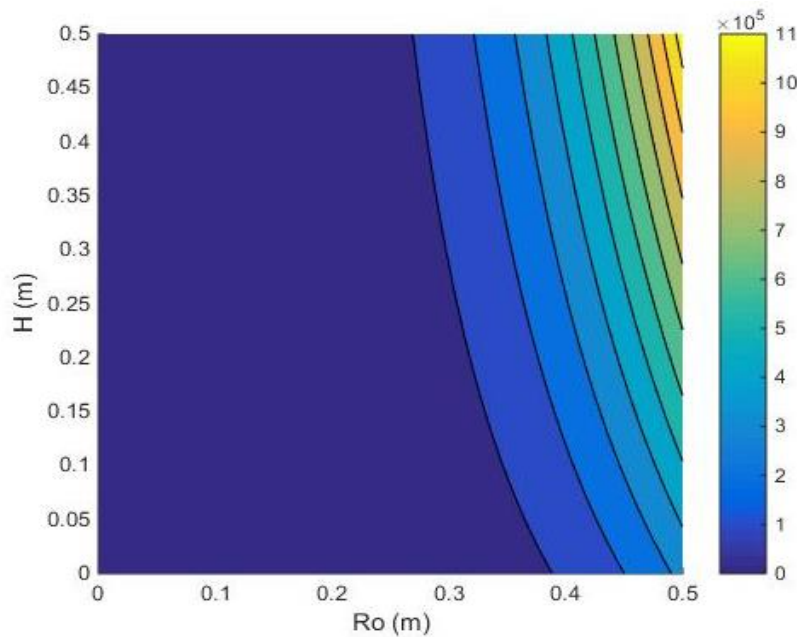
Figure: Plot showing variation of value of Pdrag with respect to R_o and H

4.4.4.2 Pre-optimization visualization of influence of variables on the power loss due to air friction

This power loss occurs due to three variables in this case the inner radius of flywheel (R_i) distance of web from top of surface container (d) and radius of shaft (r). The plot shows the variation of the inner radius of flywheel and radius of shaft for a constant value of d=0.1 m which is taken from literature. The XY plot is obtained by finding variation of Power loss due to air friction with respect to inner radius of flywheel for different values of the inner radius shaft. It is vital point to observe that for a low value of inner flywheel and for a very large value of shaft radius the value is negative, this is infeasible from which an simple geometric constraint can be derived i.e. the difference between inner radius of flywheel and radius of shaft should be strictly positive which is also logical.

Moreover for very small value of shaft radius the curves tend to overlap showing that beyond a particular value the reduction in radius of shaft has minimal influence on the power loss due to air friction and inner radius of flywheel plays a major part. From this we can conclude that we have a minimum value for shaft radius beyond which it plays a very less influence on power loss due to drag.

Figure: Plot showing variation in the air friction loss due to Inner radius of flywheel and shaft radius

4.4.4.3 Simplification of objective and constraints

The derivation for the objective function is given under section 4.4.3 after which the values of the constant are substituted for further simplification of the objective function. For the constraints the simplification done for other subsystems apply to this too and have been used as such.

4.4.4.4 Trade-off in variables

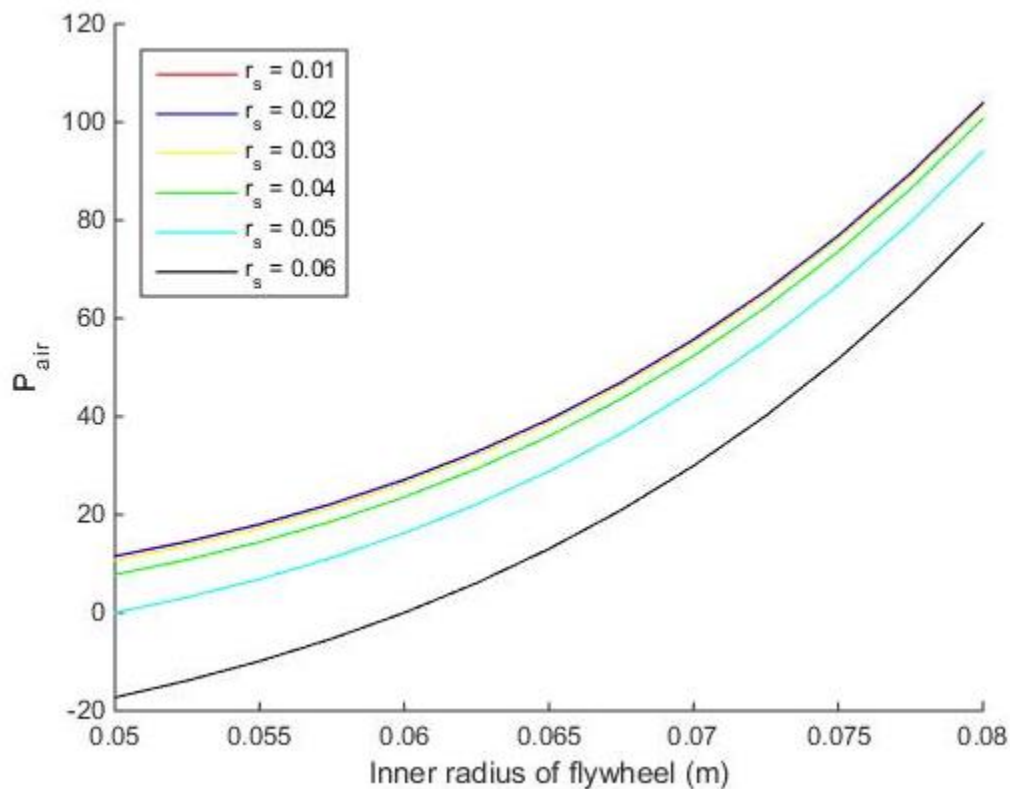In this particular system, the trade-off between the variables to other systems are significant. If the outer radius is increased then my drag loss will increase rapidly and hence my outer radius must be as small as possible. Though height of flywheel has very less effect on the drag effect but increase of this variable also amounts to increase in drag losses. But for the system where kinetic energy is to be maximized, the radius must be large to store lot of energy. Thus we must optimize in such a approach that the energy is maximized for a minimal loss due to drag force.

4.4.4.5 Monotonicity table and Active constraint

A Monotonicity analysis was conducted for all constraints with respect to the variables to obtain information on the effect on variables on the constraints and objective. In this analysis, a positive sign means that the function is increasing with the increase of variable value and negative means the vice versa. If the variables do not influence the functions then they are indicated by a '*' symbol.

It can be observed that all the variables in the objective functions are constrained by at least one constraint showing it is property constrained problem for optimization analysis.

	Ro (x(1))	H (x(2))	Ri (x(3))	r (x(4))	d (x(5))
f1	+	+	*	*	*
f2	*	*	+	-	+
g1	-	*	+	*	*
g2	+	*	*	+	*
g3	*	+	*	*	-
g4	*	-	*	*	+
g5	*	*	-	+	*

For objective f1, g1 and g4 constraints are active
For objective f2, g5, g2 and g3 constraints are active

4.4.5   Optimization Study and results

4.4.5.1 Lower and Upper bounds of the Design Variables

Variables	Lower Bound	Upper Bound
R_i	0	inf
R_o	0	inf
r	0.01	inf
d	0	inf
H	0	**0.3**

The upper bound for the height of the flywheel is vital as this constrains my objective, if upper bound is not given there is a problem arise, it makes the H value too large and R_o very small in order to satisfy my volume constraints, but in real time this is not feasible. The Flywheel was optimized for a maximum angular velocity of 30000 rpm.
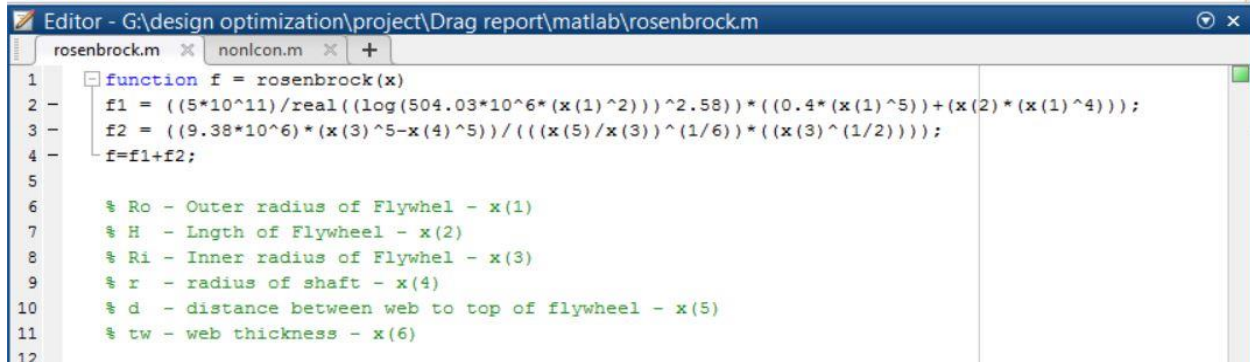
The lower bound on the radius of shaft is also very important, if lower bound is not given it makes Ri very small (or zero) in order to make the cylinder attached to shaft.

4.4.5.2 Optimization procedure

The optimization was done using the fmincon optimization app. This was used because the solution to this subsystem can be narrowed down to a particular point where we can obtain an optimal value for all the variables. The objective function is well constrained and bounded hence using the standard solver to get the optimal solution is feasible. The objective and constraint are given as inputs as functions and the bounds and linear constraints are given in the form of matrix. The solutions were also found for different algorithms like interior points, SQP and Active set with different initial points. It was found that the number of iterations were different but the results were quite the same in each algorithm used.

4.4.5.2.1   Function formulation in MATLAB

A script was created to enter the objective function, where f1 is the power loss due to drag force and f2 is loss due to air friction. The constants of the equations are substituted and simplified before they are entered. Moreover in the first function term we have log of a number which might have an imaginary part as the equation solved for getting this value has a quadratic term. The function value is the sum of the two individual power loss functions. A figure shows how he functions are given as input.

```
Editor - G:\design optimization\project\Drag report\matlab\rosenbrock.m
  rosenbrock.m ×   nonlcon.m ×   +
1      function f = rosenbrock(x)
2        f1 = ((5*10^11)/real((log(504.03*10^6*(x(1)^2)))^2.58))*((0.4*(x(1)^5))+(x(2)*(x(1)^4)));
3        f2 = ((9.38*10^6)*(x(3)^5-x(4)^5))/(((x(5)/x(3))^(1/6))*((x(3)^(1/2)))));
4        f=f1+f2;
5
6        % Ro - Outer radius of Flywhel - x(1)
7        % H  - Lngth of Flywheel - x(2)
8        % Ri - Inner radius of Flywheel - x(3)
9        % r  - radius of shaft - x(4)
10       % d  - distance between web to top of flywheel - x(5)
11       % tw - web thickness - x(6)
12
```
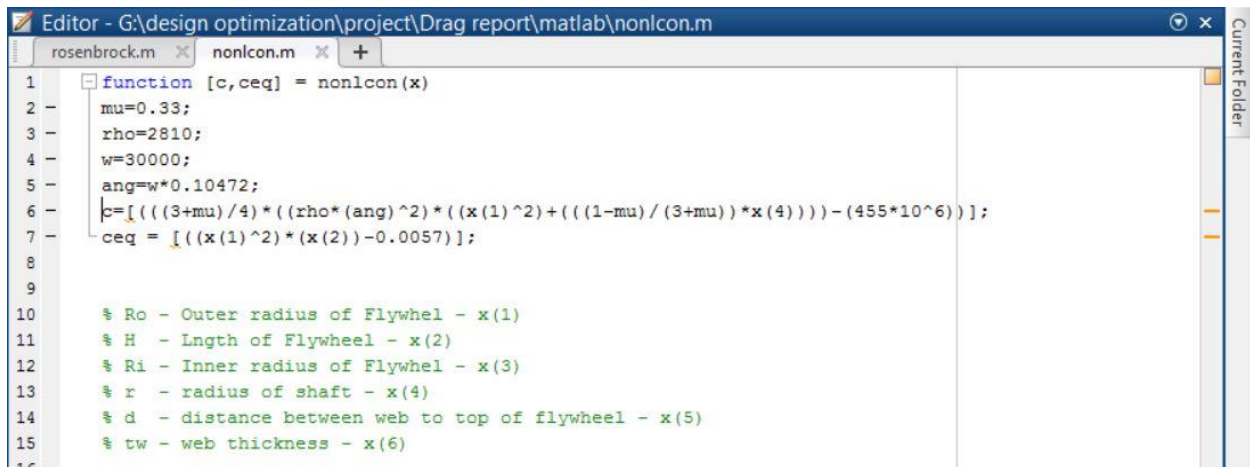
Figure: Function file for objective equation for fmincon analysis

.

4.4.5.2.2   Constraints function in MATLAB

A MATLAB file for inputting non-linear constraints were created. The stress constraint and volume constraint are inputted in the respective equal and inequality constraints sections. The material constant along with the maximum speed for the system is inputter and saved as nonlcon function file.


```
Editor - G:\design optimization\project\Drag report\matlab\nonlcon.m
  rosenbrock.m ×   nonlcon.m ×   +
1      function [c,ceq] = nonlcon(x)
2        mu=0.33;
3        rho=2810;
4        w=30000;
5        ang=w*0.10472;
6        c=[(((3+mu)/4)*((rho*(ang)^2)*((x(1)^2)+(((1-mu)/(3+mu))*x(4))))-(455*10^6))];
7        ceq = [((x(1)^2)*(x(2))-0.0057)];
8
9
10       % Ro - Outer radius of Flywhel - x(1)
11       % H  - Lngth of Flywheel - x(2)
12       % Ri - Inner radius of Flywheel - x(3)
13       % r  - radius of shaft - x(4)
14       % d  - distance between web to top of flywheel - x(5)
15       % tw - web thickness - x(6)
16
```

Figure: Function file for non-linear constraint equation for fmincon analysis

4.4.5.2.3   Optimization toolbox

The optimization was done on fmincon toolbox in the optimization tab in MATLAB, which can be used if we have to find a single point solution and if the problem is well bounded and constrained. The toolbox gives us many options to use different algorithms like SQP, Active set, interior points. An initial point must be given as input to start the iteration. The objective function and nonlinear constraints we created must be give as input in corresponding sections. Other linear constraints can be given in matrix form in the respective spaces depending on whether it is linear or nonlinear equation. The linear constraints must be given as matrix in the order of variables in which they are inputted in the rest of the simulation. In this subsystem, it is in the form [Ro,H,Ri,r,d] and right side should be the value say lesser than or equal to zero, if there is a value or it is strictly lesser than

46

zero then the corresponding value must be filled. The blonds discussed in the model analysis are given and the optimizer is run to obtain the results.
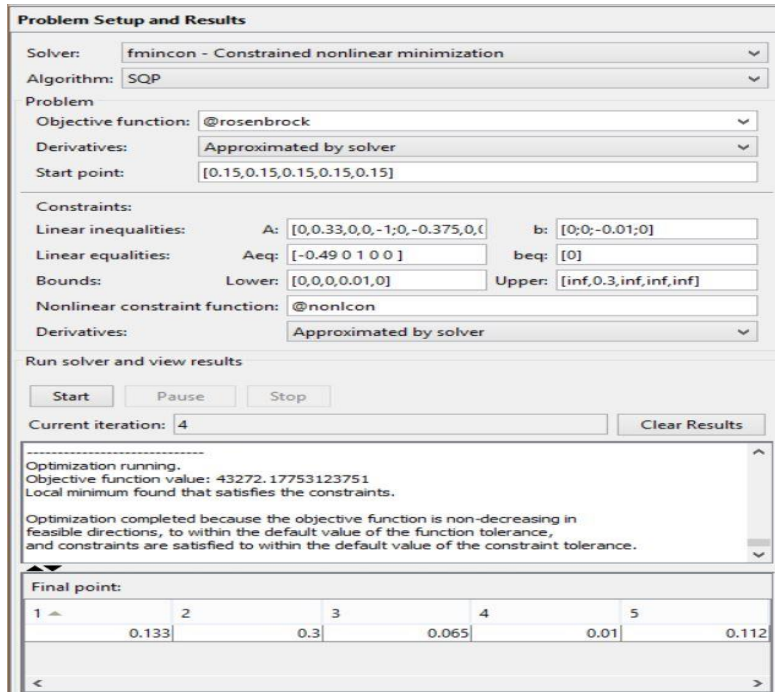
Figure: Problem setup and results for fmincon analysis

4.4.5.2.4 Global vs local

For different algorithm and different starting point, the results obtained were the same thus indicating the solution reached is a global minimum. The value of the variables varies only marginally for some staring point and does not vary for most of the starting point showing it has reached a global optimal value.

4.4.5.2.5 Discussion of Results

The results from fmincon for different variables for this subsystem is shown in the table below.

Variables	Value
R_i	0.138
Ro	0.068
r	0.058
d	0.112
H	0.3

47

From these results we can infer that radius of shaft is close to 0.06 which has very small value of power loss for the corresponding inner radius of flywheel of 0.07 m. This also shows that the value of H is hitting the upper bound and there should be more constraints in case we have to remove the bound.

Optimization plots
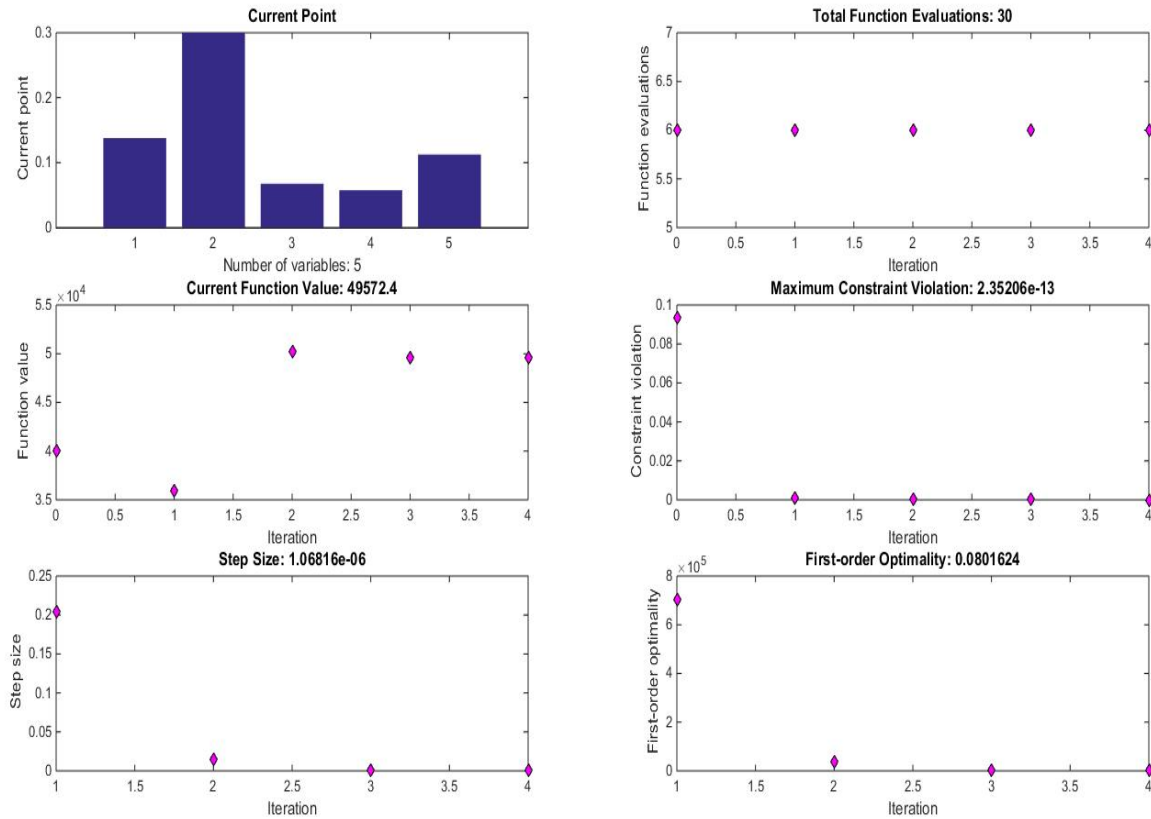
The above figure contains the details of the optimal points, Number of function evaluations required and the optimal function value.

As we have seen earlier the optimal value does not change for different initial values showing that we have reached a global optimal. The dimensions we obtained for this system are reasonable which can be concluded by evaluating the total loss in the system which is about 43 Kw of power which is manifolds the other showing it is primary loss in the flywheel.

5. System Integration

5.1 Problem statement

In previous sections, optimization study for each subsystem has done successfully and optimal results have been achieved. In this section we are going to integrate all the subsystems in order to find the optimal results for the whole system. As you see in previous sections there are several common variables between all the subsystems and there are some special variables for each subsystem. For the sake of integration we are going to use those common variables as variables and set all the special variables of each subsystem as a constant parameters for the integrated system optimization problem.

5.2 Mathematical Model

5.2.1 Objective function

Among all four subsystems, three of them deal with different kinds of energy loss and one of them deals with energy stored in system. For the integration of the systems, we decide to set the objective function described in section 1 as the whole objective function. Beside all the constraints used by this objective function in section 1, we add all other three subsystems described in section 2 through 4 as constraints.

$$KE = \frac{1}{2} I_p [\omega_{max}^2 - \omega_{min}^2]$$

5.2.2 Constraints

In Table 1 lists all the constraints used in overall optimization of system.

Constraint	Type	equation
g_1	Losses due to vibrations in coupling (Subsystem 2)	$\Delta.K.E = \left[\frac{1}{2}I_2\dot{\theta_2}^2(0)\right]$ $-\left[\frac{1}{2}I_1\dot{\theta_1}^2(t) + \frac{1}{2}I_2\dot{\theta_2}^2(t)\right]$
g_2	Losses due to magnetic bearing (Subsystem 3)	$P_{fe} = K_h f B_m^a + K_{el} f B_m$
g_3	Losses due to other mechanical losses (Subsystem 4)	$P_{drag} = \rho_a \pi\, C_{df}\, \omega^3 \left(\frac{2}{5} R_o^5 - H R_o^4\right)$ $+ \frac{\left(K_f \rho_a\, C_f\, \omega^3 (R_i^5 - r^5)\right)}{2}$
g_4	Material strength	$\frac{3+\mu}{4} \rho \frac{v}{R_o} \left(R_o^2 + \frac{1-\mu}{3+\mu} r^2\right) < S_y$
g_5	Volume constraint	$H\pi R_o^2 - 0.013 = 0$
g_6	Geometric constraint	$R_i - 0.49 R_o = 0$
g_7	Geometric constraint	$t_w - 0.2H \geq 0$
g_8	Geometric constraint	$t_w - 0.4H \leq 0$

Table 1: Constraints of the system

5.2.3 Variables and parameters

There are five variables for the whole system which is common among all subsystems. The parameters for the system are those parameters used by the subsystem described in section 1 plus all those special variables of each subsystem. In table 2 and 3 you could see variables and parameters used in this system.

Design variables	Symbol	Notations in codes	Unit
Inner radius of the flywheel	R_i	X(1)	m
Outer radius of the flywheel	R_o	X(2)	m
Radius of the shaft	r	X(3)	m
Length of the flywheel	H	X(4)	m
Thickness of the web	t_w	X(5)	m

Table 2: List of variables

Design parameters	Symbol	Unit	Values and material used
Moment of inertia of the CVT	I_2	Kg/m^2	0.21 / steel 4330
Density of the material used for flywheel	ρ	Kg/m^3	2810 / Aluminum
Poisson's ratio of the material is used for flywheel	μ	--	0.3 / Aluminum
Yield strength of the material is used for flywheel	S_y	MPa	455 / Aluminum
Equivalent spring constant of the coupling	K	N.m/rad	170
Equivalent damping coefficient of the coupling	C	$Kg.m^2/s$	0.83

Table 3: List of parameters

5.3 Optimization study

For the optimization of the integrated system, we used optimization toolbox in MATLAB and used three different algorithms under *fmincon*.

We tested different initial guesses and the optimal results for each initial guess was same. In Table 4 would see the initial guess used for all algorithms and in table 5 below that you could see the optimal results for each algorithms.

	R_i	R_o	r	H	t_w
Initial Guess	0.5	0.5	0.5	0.5	0.5

Table 4: Initial guess used in optimization tool

	Iterations	R_i	R_o	r	H	t_w
Interior Points	262	0.068	0.138	0.047	0.299	0.096
Active Set	8	0.069	0.14	0.042	0.29	0.116
SQP	18	0.069	0.14	0.042	0.29	0.116

Table 5: Optimal results for three different optimization algorithms

5.4 Discussion of the results

We tried many different initial points besides those values in table. With all those initial guesses will reached the same optimal results for each algorithms. It means at the moment we have reached global minimum for our problem.

By looking table we could see all the results based on these three different algorithm are almost the same. The only thing that is different for each algorithm is the number of iterations.

6. Parametric Study

We have considered Aluminum as the material for the flywheel. The other possible materials are Titanium, Steel, composite materials like Carbon-epoxy, etc. For the present study we considered Titanium and steel in addition to Aluminum. The properties of these materials and the corresponding energy values are given below

Material	Poisson's Ratio	Density	Mol (Kgm²)	Energy (MJ)
Aluminum	0.33	2810Kg/m³	0.4634	0.816
Titanium	0.32	4430kg/m³	0.4525	0.803
Steel	0.305	7800Kg/m³	0.2909	0.516

Table 5 Material properties for parametric study

Our project is based on Aluminum flywheel. The value of angular speed considered was 30000 rpm. The calculations were also carried out for different values of rpm. The rotational speeds were chosen over a range from 20000 rpm to 30000 rpm. The influence of this variation on the energy stored is shown in the below plot.
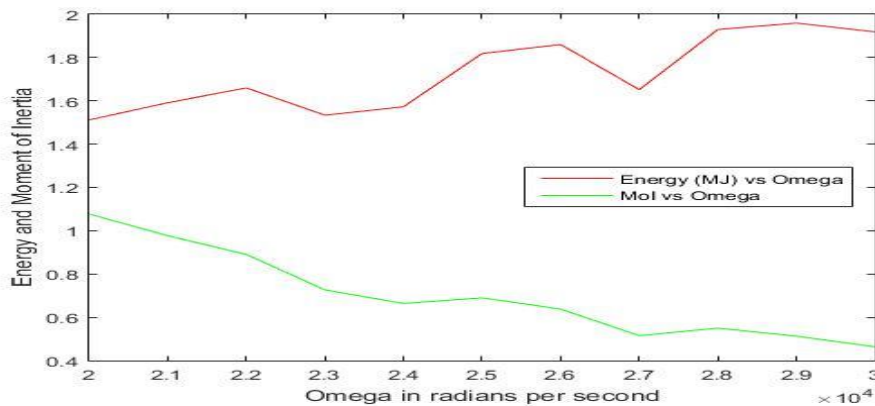

Figure: Variation of energy and moment of inertia with respect to angular velocity

From the above plot we can conclude that in general, with the increase in the rotational speed of the flywheel, the energy stored is increasing. But the graph also makes a strong statement that though the moment of inertia is decreasing throughout the increase in omega, there is still an increase in stored energy. This is because the energy varies directly with the moment of inertia and the square of the rotational speed. So the change in rotational speed will have greater effect on the energy stored in the flywheel system.

By varying the initial points and solving the optimization problem, it can be observed that the variables and the objective function value changes only by a small margin. This shows that the local minima obtained by solving this optimization problem is the global minima.

Optimization results after system integration

For initial points [0.1;0.1;0.1;0.1;0.1]

```
x =

    0.0686    0.1400    0.0239    0.2924    0.1170


fval =

   -0.4782
```

For initial points [0.2;0.2;0.2;0.2;0.2]

```
x =

    0.0686    0.1401    0.0203    0.2920    0.1168


fval =

   -0.4790
```

For initial points [0.05;0.05;0.05;0.05;0.05]

```
x =

    0.0685    0.1398    0.0288    0.2932    0.1170


fval =

   -0.4767
```

For initial points [0.5;0.5;0.5;0.5;0.5]

```
x =

    0.0685    0.1398    0.0246    0.2932    0.1173


fval =

   -0.4770
```

7. Conclusion and future work

For each subsystem we got optimal results based on objective functions and corresponding constraints. Although these values were different for each subsystem, they were in a reasonable domain that showed all objective functions and constraints have defined well. Also the differences between the optimal values of the variables show that there might be some contradictions between optimal results of each subsystem.

As described in section 5, we integrated all subsystems together in order to find final optimal results for the whole system. For this matter we used the objective function of the structural subsystem as an overall objective function and set all other objective functions as constraints for that objective function.

The final results that we got as optimal points didn't match exactly any optimal values of subsystems but the optimal results were close enough to them. This thing presents that there is a tradeoff between optimal results of each subsystems when they are combined together.

This project has thrown us some insight on influence on variation of important parameters of flywheel. This project gave us knowledge on how to break a complex system in subparts and recombine them to optimize with a particular objective. Being a very new technology it has very limited recourses about the details, if more constraints are added a better optimization can be done

Speed	Obtained results	Actual results	Obtained Results	Actual Results
20000	I=0.4593 Energy=0.161 KJ		Ro=0.1379 m Ri=0.0676 m r= 0.047 m H= 0.299 m Tw= 0.096 m	Ro= 0.14 m Ri= 0.07 m r= 0.06 m H= 0.30 m
30000	I=0.4593 Energy=0.816 MJ	I=0.45 Energy=0.8 MJ	Ro=0.1379 m Ri=0.0676 m r= 0.047 m H= 0.299 m Tw= 0.096 m	Ro= 0.14 m Ri= 0.07 m r= 0.06 m H= 0.30 m

8.   Reference

[1]   Jerome Tzeng, Ryan Emerson, Paul Moy "Composite flywheels for energy storage" Composites Science and Technology 66 (2006) 2520–2527.

[2]   "An Assessment of Flywheel High Power Energy Storage Technology for Hybrid Vehicles" Oak Ridge National Laboratory, Department of Energy

[3]   Johan Abrahamsson, Janaína Gonçalves de Oliveira, Juan de Santiago, Johan Lundin and Hans Bernhoff "On the Efficiency of a Two-Power-Level Flywheel-Based All-Electric Driveline" Energies 2012, 5, 2794-2817.

[4]   Baoquan Kou, Haichuan Cao, Da Zhang, Weili Li and Xiaochen Zhang, "Structural Optimization of High Speed Permanent Magnet Synchronous Motor for Flywheel Energy Storage", Electromagnetic Launch Technology (EML), 2012.

[5]   E. Maleki Pour, S. Golabi "Design of Continuously Variable Transmission (CVT) with Metal Pushing Belt and Variable Pulleys" International Journal of Automotive Engineering Vol. 4, Number 2, June 2014

[6]   Alan Westbay "Flywheel Energy Storage and Release via Continuously Variable Transmissions" 2014 ASEE Southeast Section Conference

[7]   Shaobo Wen "Analysis of maximum radial stress location of composite energy storage flywheel rotor" Arch Appl Mech (2014) 84:1007–1013

[8]   S. K. Ha, S. K. Choi, D. J. Kim and I. J. Chin "Stress Analysis of a Hybrid Flywheel Rotor Using a Modified Generalized Strain Assumption" Composites: Part B 33 (2002) 433–459.

[9]   S.M. Arnold, A.F. Saleeb, N.R. Al-Zoubi "Deformation and life analysis of composite flywheel disk systems"

[10]   Johan Abrahamsson *, Janaína Gonçalves de Oliveira, Juan de Santiago, Johan Lundin and Hans Bernhoff "On the Efficiency of a Two-Power-Level Flywheel-Based All-Electric Driveline" Energies 2012, 5, 2794-2817

[11]   Malte Krack, Marc Secanell and Pierre Mertiny "Rotor Design for High-Speed Flywheel Energy Storage Systems"

[12]   Sheng Xu "Design and Prototyping of a Low-Speed Flywheel System for Automotive Brake Energy Recovery"

APPENDIX

I: STRUCTURAL SUBSYSTEM

1. Objective Function

```
function f =rosenbrock(x)
rho=2810;
f=-(((1/2)*rho*pi)*((x(4)*(x(1)^4-x(3)^4))+(x(5)*(x(2)^4-x(1)^4))));
```

2. Non Linear Constraint Equations

```
function [c,ceq] = unitdisk(x)
mu=0.33;
omega=3141.59;
rho=2810;

c=[(((((3+mu)/4)*(rho*((omega)^2))*((x(2)^2+((1-mu)/(3+mu))*x(3)^2)))-455000000)];
ceq=[x(5)*pi*(((x(2))^2))-0.018];
```

3. Radius Ratio vs Specific Energy and Energy Density plot

```
x=[0;0.1;1];
y1=((400^2)/4)*(1+x.^2);
y2=((2810*(400^2))/4)*(1-x.^4);
figure
set(gca,'FontSize',20)
[hAx,hLine1,hLine2]=plotyy(x,y1,x,y2);
grid on;
xlabel('radius ratio')
ylabel(hAx(1),'specific energy','FontSize',20);
ylabel(hAx(2),'energy density','FontSize',20);
legend('y1 = specific energy','y2 =energy density ')
```

4. Inner Radius vs moment of inertia and mass of the flywheel

```
rho=2810;
h=0.292;
R=[0.1:0.05:0.5];
r=0.49*R;
f=(((1/2)*rho*pi)*(h)*((R.^4)-(r.^4)));
g=(h*pi*((((R-r).^2))))*rho;
set(gca,'FontSize',20)
[hAx,hLine1,hLine2]=plotyy(r,f,r,g);
ylabel(hAx(1),'Moment of inetia','FontSize',20);
ylabel(hAx(2),'mass of the flywheel','FontSize',20);
legend('y1 = specific energy','y2 =energy density ')
xlabel('inner radius ')
```

5. Contour plot determining the relationship between the inner and outer radius and the moment of inertia of the flywheel

```matlab
rho=2810;
h=0.292;
R=[0.1:0.05:0.5];
r=0.49*R;

for x1=1:length(R)
    for y1=1: length(r)
        x2d(x1,y1)=R(x1)
        y2d(x1,y1)=r(y1);
        f(x1,y1)=(((1/2)*rho*pi)*(h)*((R(x1)^4)-(r(y1)^4)));


    end
end
hold on
figure(1)
contourf (x2d,y2d,f);
axis equal
xlabel ('R (m)');
ylabel ('H (m)');
```

II: VIBRATION SUBSYSTEM

1. Objective function

```matlab
function f = objective(x)

rho = 2810;

% Tw = x(1);
% H = x(2);
% Ri = x(3);
% Ro = x(4);
% r = x(5);
% K = x(6);
% C = x(7);

[t,a,b,c,d] = Sys4ODEsRK4(@TorsionalDthetaOneDt,...
    @TorsionalDthetaTwoDt,@TorsionalDwDt, @TorsionalDuDt,...
    0,6.67,0.1,0,0,0,3140,x);
theta1dot = c(end);
f = -((1/2)*((1/2)*rho*pi)*((x(1)*(x(3)^4 - x(5)^4)) + (x(2)*...
    (x(4)^4-x(3)^4))) * theta1dot^2);

End
```

2. Linear constraints / initial guesses / lower bound, upper bound

```
x0 = [0.04, 0.04, 0.08, 0.1, 0.03, 170, 0.45];
A = [0 0 1 -1 0 0 0; -1 0.2 0 0 0 0 0; 1 -0.4 0 0 0 0 0; 0 0 -1 0 1 0
0]; %
b = [0.001; 0; 0; 0.07]; %
Aeq = [0 0 1 -0.49 0 0 0];
beq = 0;
lb = 0.01*ones(7*1);
ub = 500*ones(7*1);
```

3. Nonlinear constraint

```
function [g , h] = nonlincond(x)

Sy = 455e6;
Mu = 0.33;
rho = 2810;
v = 1000;

% Tw = x(1);
% H = x(2);
% Ri = x(3);
% Ro = x(4);
% r = x(5);

g = ((3+Mu)/4)*rho*((v/x(4))^2)*(x(4)^2+((1-Mu)/(3+Mu))*x(5)^2) - Sy;
h = x(2)*(x(4)^2)-0.0041;
end
```

4. Fourth order Runge-Kutta method for solving ODEs

```
function [t,a,b,c,d]=Sys4ODEsRK4(ODE1,ODE2,ODE3,ODE4,A,B,h,a1,b1,c1,d1,x)
% Sys2ODEsRK4 solves a system of two first-order initial value ODEs usinq
% fourth-order Runqe-Kutta method.
% The independent variable is t, and the dependent variables are x and y.
% Input variables:
% ODE1 Name for the function that calculates da/dt.
% ODE2 Name for the function that calculates db/dt.
% ODE3 Name for the function that calculates dc/dt.
% ODE4 Name for the function that calculates dd/dt.
% x The first value of t.
% y The last value of t.
% h The size of a increment.
% a1 The initial value of a.
% b1 The initial value of b.
% c1 The initial value of c.
% d1 The initial value of d.
% Output variables:
% t A vector with the t coordinate of the solution points.
% a A vector with the a coordinate of the solution points.
% b A vector with the b coordinate of the solution points.
% c A vector with the a coordinate of the solution points.
```

```matlab
% d A vector with the b coordinate of the solution points.
t(1) = A; a(1) = a1; b(1) = b1; c(1) = c1; d(1) = d1;
n = (B - A)/h;
for i = 1:n
t(i+1) = t(i) + h;
tm = t(i) + h/2;
Ka1 = ODE1(t(i),x,a(i),b(i),c(i),d(i));
Kb1 = ODE2(t(i),x,a(i),b(i),c(i),d(i));
Kc1 = ODE3(t(i),x,a(i),b(i),c(i),d(i));
Kd1 = ODE4(t(i),x,a(i),b(i),c(i),d(i));
Ka2 = ODE1(tm,x,a(i)+ Ka1*h/2,b(i)+ Kb1*h/2,c(i)+ Kc1*h/2,d(i)+ Kd1*h/2);
Kb2 = ODE2(tm,x,a(i)+ Ka1*h/2,b(i)+ Kb1*h/2,c(i)+ Kc1*h/2,d(i)+ Kd1*h/2);
Kc2 = ODE3(tm,x,a(i)+ Ka1*h/2,b(i)+ Kb1*h/2,c(i)+ Kc1*h/2,d(i)+ Kd1*h/2);
Kd2 = ODE4(tm,x,a(i)+ Ka1*h/2,b(i)+ Kb1*h/2,c(i)+ Kc1*h/2,d(i)+ Kd1*h/2);
Ka3 = ODE1(tm,x,a(i)+ Ka2*h/2,b(i)+ Kb2*h/2,c(i)+ Kc2*h/2,d(i)+ Kd2*h/2);
Kb3 = ODE2(tm,x,a(i)+ Ka2*h/2,b(i)+ Kb2*h/2,c(i)+ Kc2*h/2,d(i)+ Kd2*h/2);
Kc3 = ODE3(tm,x,a(i)+ Ka2*h/2,b(i)+ Kb2*h/2,c(i)+ Kc2*h/2,d(i)+ Kd2*h/2);
Kd3 = ODE4(tm,x,a(i)+ Ka2*h/2,b(i)+ Kb2*h/2,c(i)+ Kc2*h/2,d(i)+ Kd2*h/2);
Ka4 = ODE1(tm,x,a(i)+ Ka3*h/2,b(i)+ Kb3*h/2,c(i)+ Kc3*h/2,d(i)+ Kd3*h/2);
Kb4 = ODE2(tm,x,a(i)+ Ka3*h/2,b(i)+ Kb3*h/2,c(i)+ Kc3*h/2,d(i)+ Kd3*h/2);
Kc4 = ODE3(tm,x,a(i)+ Ka3*h/2,b(i)+ Kb3*h/2,c(i)+ Kc3*h/2,d(i)+ Kd3*h/2);
Kd4 = ODE4(tm,x,a(i)+ Ka3*h/2,b(i)+ Kb3*h/2,c(i)+ Kc3*h/2,d(i)+ Kd3*h/2);
a(i+1)  = a(i)  + (Ka1 + 2*Ka2 + 2*Ka3 + Ka4)*h/6;
b(i+1)  = b(i)  + (Kb1 + 2*Kb2 + 2*Kb3 + Kb4)*h/6;
c(i+1)  = c(i)  + (Kc1 + 2*Kc2 + 2*Kc3 + Kc4)*h/6;
d(i+1)  = d(i)  + (Kd1 + 2*Kd2 + 2*Kd3 + Kd4)*h/6;
end
```

III: MECHANICAL SUBSYSTEM

1. Code for plotting power loss due to drag by varying height and radius of flywheel

```matlab
clc;
clear all;
%Constants
rho=1.127;
w=30000*0.10467;
H=0.1:0.1:0.5;
Ro=0.10:0.01:0.25;

for x=1:length(H)
   y=1:length(Ro);
   Pdrag(x,y)=0;
for y=1:length(Ro)
Re=504.03e6*((Ro(y))^2);
cd=0.455/real((log(Re))^2.58);
Pdrag(x,y)=pi*rho*(w^3)*cd*(((2/5)*Ro(y)^5)+(H(x)*Ro(y)^4));
end
end
hold on
plot(Ro,Pdrag(1,:),'-r')
plot(Ro,Pdrag(2,:),'-b')
```

```
plot(Ro,Pdrag(3,:),'-y')
plot(Ro,Pdrag(4,:),'-g')
plot(Ro,Pdrag(5,:),'-c')
xlabel('Outer radius of flywheel (m)');ylabel('P_d')
legend('H = 0.1','H = 0.2','H = 0.3','H = 0.4','H = 0.5', 'Location','northwest')
```

2. Contour plot code for power loss due to drag by varying height and radius of flywheel

```
clc;
clear all
Ro=[0:0.01:0.5];
H=[0:0.01:0.5];
rho=1.128;
v=0.70244*10^-5;
w=30000*0.10467;
for x1=1:length(Ro)
    for y1=1: length(H)
        x2d(x1,y1)=Ro(x1);
        y2d(x1,y1)=H(y1);
        Re=(rho*w*(Ro(x1))^2)/v;
        cd=0.455/((log(Re))^2.58);
        P_drag (x1,y1) = pi*rho*cd*w^3*((0.4*(Ro(x1))^5)+(H(y1)*(Ro(x1))^4));

    end
end

hold on
figure(1)
contourf (x2d,y2d, P_drag);
axis equal
xlabel ('Ro (m)');
ylabel ('H (m)');
```

3. Code for plotting variation of air friction losses

```
clc;
clear all;
%Constants
rho=1.127;
w=30000*0.10467;
%Variables
dis=0.1:0.1:0.5;          %d as variable
Ri=0.05:0.0025:0.08;    %Ri inner of flywheel
r=0.01:0.01:0.06;         %r  radius of shaft
d=0.1;                    %d as constant

for c=1:length(Ri)
```

```matlab
b=1:length(r);
Pair(c,b)=0;
for b=1:length(r)
r1=Ri(c);
r2=r(b);
Re=504.03e6*r1^2;
% for e=1:length(dis)
% d=dis(e);
cf=0.08/(((d/r1).^(1/6))*((Re)^(1/4)));
Pair(c,b)= Pair(c,b)+(cf*rho*(w^3)*(r1^5-r2^5)/(2));
% end
end
end
Pair;
% z=[0.1875:0.0025:0.3]';
hold on
plot(Ri,Pair(:,1),'-r')
plot(Ri,Pair(:,2),'-b')
plot(Ri,Pair(:,3),'-y')
plot(Ri,Pair(:,4),'-g')
plot(Ri,Pair(:,5),'-c')
plot(Ri,Pair(:,6),'-k')
xlabel('Inner radius of flywheel (m)');ylabel('P_a_i_r')
legend('r_s = 0.01','r_s = 0.02','r_s = 0.03','r_s = 0.04','r_s = 0.05','r_s = 0.06',
'Location','northwest')
```